Universidad del País Vasco / Euskal Herriko Unibertsitatea

Facultad de Química / Kimika Fakultatea

Double Master in Polymer Science (UPV/UBx)

Final Degree Project

"Circular Biobased Synthesis of Carbon Nano Dots for Agricultural Applications"

Author : Hélia Ventribout-Rodríguez (hventribout001@ikasle.ehu.eus)

Director : Haritz Sardon Muguruza

Supervisor : Gabriel Perli

San Sebastián, July 2024

Abstract

Direct consequence of the climate change crisis and global population increase, there is an imminent need of sustainable alternatives to reaching the food production required. Here, a circular biobased synthesis of carbon nanodots (CNDs) is presented. With as principal objectives the enhancing of the photosynthesis process in plants, and an alternative to the chemical pesticides, innovative ways of optimization were studied. Starting from orange peels waste biomass, an easy synthesis pathway was developed with two optimization steps. First, an N-doping process with caffeine was employed, which resulted in the integration of the N functional groups in the CNDs revealing an enhance fluorescence emission. Then, the addition of different essential oils in the process lead to the binding of the volatile organic compounds (VOCs) functional groups on the CNDs surface. The resulting CNDs present as principal features a bright blue fluorescence, a size around 7 to 8 nm with spherical shape and the integration of the desired functional groups on the surface. Finally, the insect repellency behavior of the CNDs systems against pea aphids was evaluated, resulting in encouraging results with weakly to moderate repellency effect.

Resumen

Consecuencia directa de la crisis del cambio climático y del aumento de la población mundial, existe una necesidad inminente de alternativas sostenibles para alcanzar la producción de alimentos requerida. Aquí se presenta una síntesis circular biobasada de nanopuntos de carbono (CNDs). Con el objetivo principal de potenciar el proceso de fotosíntesis en las plantas, y como alternativa a los pesticidas químicos, se estudiaron formas innovadoras de optimización. Partiendo de biomasa residual de cáscaras de naranja, se desarrolló una vía de síntesis sencilla con dos pasos de optimización. En primer lugar, se empleó un proceso de dopaje de N con cafeína, que dio lugar a la integración de los grupos funcionales N en los CNDs revelando una emisión de fluorescencia mejorada. A continuación, la adición de diferentes aceites esenciales en el proceso condujo a la unión de los grupos funcionales de los compuestos orgánicos volátiles (COVs) en la superficie de los CNDs. Los CNDs resultantes presentan como características principales una fluorescencia azul brillante, un tamaño alrededor de 7 a 8 nm con forma esférica y la integración de los grupos funcionales deseados en la superficie. Finalmente, se evaluó el comportamiento repelente de insectos de los sistemas de CNDs frente a pulgones del guisante, obteniéndose resultados prometedores con un efecto repelente de débil a moderado.

Identification and reflection on the sustainable development goals (SDGs)

The contribution of this project to the Sustainable Development Goals (SDGs)[1] of the 2030 agenda proposed by the European Union (EU) is worth being highlighted. The seventeen goals proposed are presented in Figure 1.

The global population growth lead to a significant increase in agricultural needs. As climate change is one of the main preoccupations of scientists worldwide. With extreme climates, from aridity to flooding, these changes also drastically affects the agriculture productivity. To meet their economic and productivity objectives, industrial agriculture relies on the consequent use of conventional fertilizers and pesticides. However, these traditional agricultural chemicals pose risks to human health and the environment (14, 15). Therefore, it is important to develop alternative solutions to these chemical compounds.

In this sense, this project aims to develop a possible alternative to the current pesticides used. With the use of biomass waste as starting material which limits the use of chemicals in the synthesis process. The pathway synthesis was also considered to be simple, without the use of organic solvents (6,7).

Another aspect presented is that the insect-repellency tests presented were carried out by preserving the aphids, as the carbon dots are non-toxic, and the essential oils used are organic and in very small amounts (12).

Figure 1. Sustainable Development Goals (SDGs)[1]

Index

1. Introduction

1.1. Current challenges in agriculture

The current global climate change crisis is a primary concern worldwide. Not only fauna and flora are affected by the consequences of global warming, but humans also face significant challenges due to these drastic environmental changes. Last report from the Intergovernmental Panel on Climate Change (IPCC) from March 2023[2], warns about an increase of the global surface temperature of 1.5°C by 2030, in the best scenario. What seems like a small change in temperature, actually presents an important impact on the world.

1.1.1. Increasing food demand

The United Nations organization projects that by 2050, the global population will reach nearly 10 billion people[3]. Directly correlating with an increase demand in food, next years will be decisive to achieve the needed crop productivity. Figure 2. illustrates clearly the actual challenge faced.
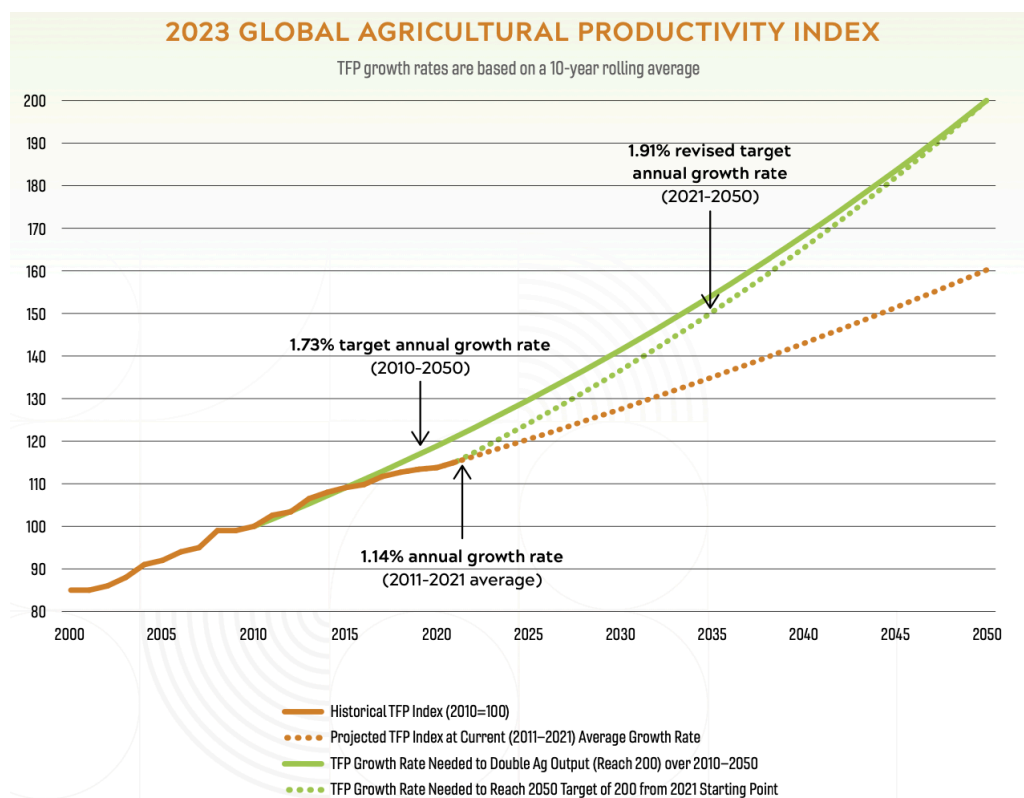

Figure 2. Current Total Factor of Productivity (TFP) and projections until 2050[4]

Between 2000 and 2015, displayed in the first part of the graph, the annual growth rate of the TFP reached the projected and needed growth rate. Whereas, since 2015, the tendency differs showing a gap between the target annual growth rate and the projected one (1.91 and

1.14%, respectively). With the increasing global population and methods of production, the food demand will not be achieved. In this perspective, diverse and numerous scientific research are carried out, to find viable and sustainable solutions.

Actual inequalities between regions of the world are well known, as some regions suffer droughts, like the south of Spain and many other places, others as subjected to impressive floods. These intensive changes provided by the elements are among the unforeseeable consequences endured by the agricultural industry, leading to important difficulties into reaching the necessary crop productions projected. Even with the new technologies employed nowadays to improve the productivity and yields, the potential of the croplands is not achieved[5].

1.1.2. *Conventional pesticides and fertilizers*

Contemporary agricultural techniques prioritize high yields through the use of chemical fertilizers and pesticides, known to present risks to both ecosystems and human health.

Since 1939, with the highlighted insecticidal properties of DDT (dichlorodiphenyltrichloroethane)[6], synthetic pesticides have emerged as an efficient solution against most pests present in fields. From the point of view of farmers and industries, pesticides are essential to prevent diseases or infestations, that could lead to significant losses in terms of food waste and economy[7]. But a large number of scientific research also refers to the hazards of this pesticides, and an urgent need to develop alternative sustainable solutions.

Conventional pesticides can be classified in different groups as organophosphates, cyclodienes and organochlorines[8] (Figure 3). Apart from the efficiency of these chemicals to face pests, their intensive use is a current problematic. The consequences engendered on the soils are disastrous and nearly irreversible. Toxic substances present in pesticides can stay in soils for years after their use, causing millions of microorganisms contained in the soils to disappear[9].
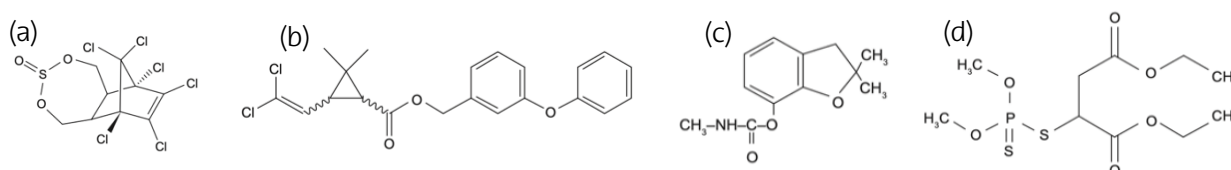

Figure 3. Examples of chemical structure of conventional pesticides, (a) Endosulfan (Organochloride), (b) Permethrin (Pyrethroid), (c) Carbofuran (Carbamate) and (d) Malathion (Organophosphate)[10]

For the last 50 years, fertilizers have been used in crop fields with the objectives of providing macro and micronutrients to the plants and increasing the efficiency and yield of the production. The most used conventional fertilizers are urea, triple phosphate, diammonium phosphate or nitrogen phosphorous potassium [11]. A rise in the use of this fertilizers has been reported by the International Fertilizer Industry Association (IFIA) in the last few years. As well as for pesticides, the intensive use of fertilizers can lead to an overdosing of the chemical compounds and consequently to environmental issues.

1.1.3. Nutrient content in food

Essential aspect of the fruits and vegetables produced in the world, these last decades the content in nutrients tends to decrease. Lobbyist of the food-processing industry take more interest into the economical profits, than into the quality of the food. Resulting in the use of more and more chemicals for a high yield productivity. The most common fruits such as oranges, apples or mangos lost their nutritional density by up to 25-50% [12].

Other than undernutrition challenges that occur daily in a lot of regions of the world, a great part of the global population is also confronted to malnutrition, presented as a lack of nutriments in the consumed food. Mineral nutrients as N, K, Mg, P, Cu or Zn, are all essential for the vitality and good functioning of the human body. A study carried out in the UK [13], showed reductions in sodium, calcium and other minerals content in the food produced by the country and imported. This nutrient composition changes observed can be related to the outbreak of high-yielding varieties and the shift from natural to conventional farming.

In this purpose, Carbon Dots appear as a newly sustainable possible alternative to conventional pesticides and fertilizers. With various known properties as photoprotection, antifungal and potentially insect-repellent, this nanomaterials also present remarkable photoluminescent properties. By allowing the plants to absorb in a broader UV range, the photosynthesis process is enhanced. The possibilities offered by CNDs are really considered with the aim of a more sustainable world[14].

1.2. Carbon Nano Dots : synthesis, properties and applications

Accidentally discovered in 2004 [15], Carbon Dots can be defined as a carbon-based nanomaterials, with a size of particle usually lower than 20 nm. Carbon Dots is a general term that includes different types of nanoparticles. These nanoparticles are composed of a carbon core and superficial functional groups.
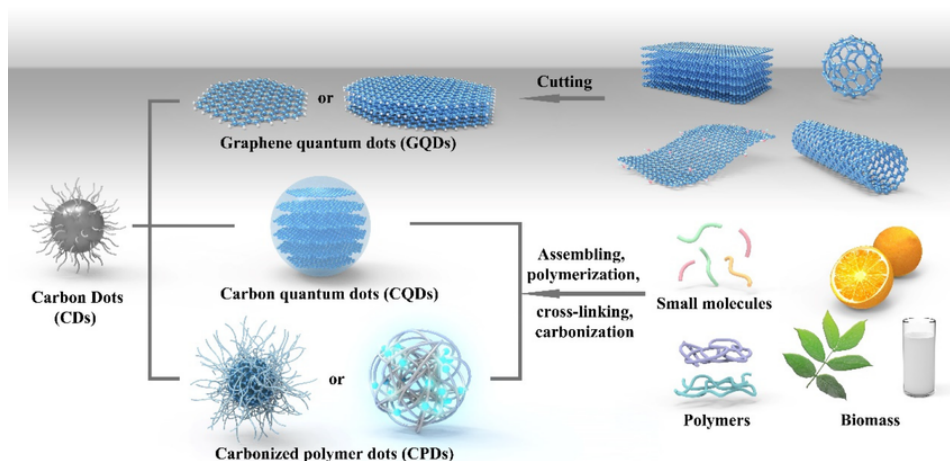

Figure 4. Classification of CDs[16]

As presented in Figure 4, the three main types of CDs are graphene quantum dots (GQDs), carbon quantum dots (CQDs), and carbonized polymer dots (CPDs). The difference between them is mainly based on the ways of preparation and the starting material used. The final structure of these nanoparticles also differs.

1.2.1. *Starting materials and synthesis methods*

Carbon is an omnipresent element that plays a fundamental role in natural and synthetic processes. Usually, this type of carbon nanomaterials is obtained from petroleum based components or natural gas, which leads to high carbon dioxide emissions and a dependence on non-renewable resources[17]. More recent studies also propose synthesis methods starting from polymeric materials, leading to CDs with very interesting properties.

Different methods are used to synthesize those nanoparticles, which are classified into two approaches : bottom-up and top-down [18](Figure 5).

Top-down method relates to breaking down large carbon structures, mainly by chemical, electrochemical, or physical routes. As precursors, graphite, carbon fibers and carbon black can be used. The different techniques used in this method are chemical ablation,

chemical oxidation, or arc discharge. The starting materials used are expensive, and the methods include long reaction times.

Bottom-up approach consists of converting smaller molecules composed of carbon structures into CDs, allowing more synthesis possibilities. The most commonly used techniques for this approach are hydrothermal treatment, microwave synthesis, pyrolysis, or thermal decomposition.
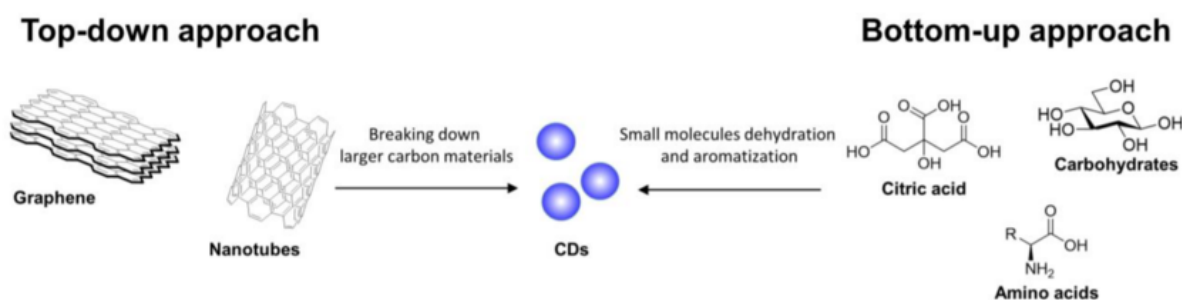

Figure 5. Schematic representation of top-down and bottom-up synthetic approaches for the preparation of CDs[19]

1.2.2. Photoluminescence mechanisms and CNDs properties

CNDs exhibit fluorescence owing to their unique electronic and structural properties at the nanoscale level. The basis mechanism of fluorescence includes three main steps that can be illustrated by the Jablonski diagram (Figure 6)[20].
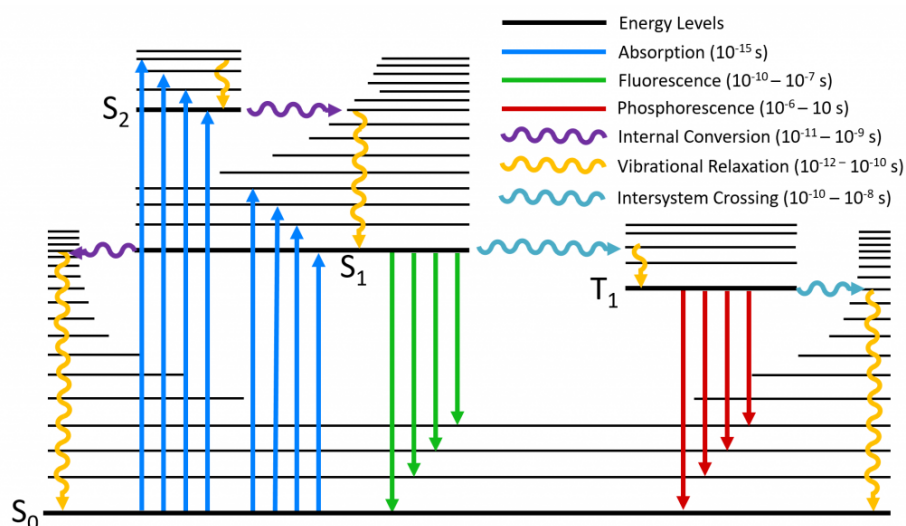

Figure 6. Jablonski diagram

Absorption, also called excitation occurs when the nanoparticles, by exposition to UV light, absorb a photon resulting in the transition from a ground state energy level to a higher

energy state (blue arrows on Figure 6). In a same electronic state (S) different levels appear called vibrational levels. Once the nanoparticles transitions to a higher state it is no longer in equilibrium and will find a way to dissipate its energy. One of this ways is through vibrational relaxation (yellow arrows in Figure 6), transitioning to a lower vibrational levels but in the same excited state. The dissipation of energy can also happen via internal conversion and is qualified as non-radiative transition. The last step is the radiative transition also called emission that leads to the fluorescence of the CNDs (green arrows in Figure 6). It is presented as the transition from a higher level state to the ground state, resulting in an emission.

In addition to the Jablonski diagram presenting the basic mechanism of fluorescence, the specific case of CNDs present other possible mechanisms to explain their reliable photoluminescent properties. Different hypothesis of the possible mechanisms responsible of this noticeable fluorescence have been exposed. The main aspects responsible of this fluorescence are surface defects and quantum confinement effect [21,22]

The quantum confinement effect manifests when carbon materials are diminished to nanoscale dimensions, causing electrons and holes to be confined within a small volume, generating discrete energy levels. Upon absorbing energy, such as light, these confined electrons transition to higher energy states and subsequently emit light upon returning to the ground state, resulting in fluorescence [17,23].

Additionally, chemical composition of CNDs composed of functional groups, like carboxyl, hydroxyl, and amino groups, present on the surface contribute to the fluorescence effect by introducing localized electronic states. In this case, the fluorescence resulting is not due to the functional groups themselves, but to the link between these groups and the core-shell[24].

Even if fluorescence is the most visible property of CNDs, this nanomaterial exhibits various other qualities. CDs present a very low toxicity (in low dosages), useful property for biological and biomedical[25] applications. Electrical properties, photostability and low cost can also be mentioned[26].

1.2.3. Applications

In the last 20 years since their discovery, carbon dots intrigue the scientific field, as nanotechnologies in general, brought a new vision and perspective in various domains.

Biomedical applications[27] have been of great interest for the scientific field. Due to their biocompatibility[28] and optical properties, they present encouraging results in

bioimaging. For example, in cancer cells imaging, with their nanoscale size they are able to enter rapidly the cells through different body tissues and help medical teams to identify the disease. Furthermore, the possibility to functionalize these nanoparticles is a huge advantage in metal ions detection based on the changes on fluorescence intensity[29].

Solar cells[30] also welcomed CDs into their field, as the optical properties are of interest in this application. Used as an alternative to noble metals, CDs can present different uses for solar cells performance. They offer the possibility to be dissolved and arranged as a thin layer on the cells, increasing their efficiency. This purpose of rare-earth metals substitution can also be appreciated in optical fibers[31] cavities.

1.2.4. *New starting materials*

However, it can be highlighted that efforts have been made to synthesize carbon materials from biomass, being and abundant and non-edible source derived from various plants sources, including herbs, wood or fruits and vegetables waste.

The synthesis of carbon nanomaterials from waste biomass can offer a green and circular approach to meeting agricultural needs. For example, by using waste biomass from the food-processing industry, the discarded biomass can be valorized into biocompatible CNDs.

The main objective of this project is to develop a sustainable method to synthesize CNDs. The first requirement to consider is the selection of the starting material. In addition to being a source of carbon, the biomass used as a starting material needs to have other characteristics, like being biobased, renewable, non-edible, abundant, and affordable.

Fruit biomass waste is an option that has been developed in different research projects on carbon nanoparticle synthesis [32–34]. According to Spain's Department of Agriculture [35], Spain is now the world's major exporter of citrus, with a main production of oranges. However, this production is being slowed down by increasing aridity, especially on the Mediterranean coast and the south of the peninsula.

In addition, orange peels are an evident waste today that represent approximatively 20% of the fruit . The reuse of this biomass to synthesize CNDs, can be engraved in a future circular project to boost the productivity of Spanish fields that suffer the consequences of climate change.

The composition of orange peel (Figure 6) is very interesting as a carbon source. Mostly composed of pectin, hemicellulose, and cellulose, those polysaccharides are mainly formed of carbon cycles with oxygen bonds, with hydroxyl and acid groups attached.
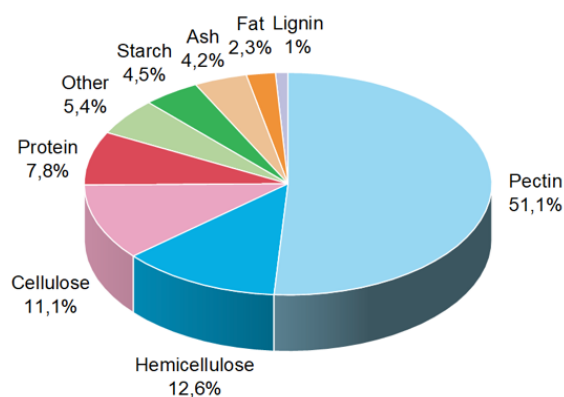

Figure 7. Chemical composition of orange peel on dry matter basis[36]

1.3. Chemical modification of CNDs

As mentioned above, functional groups present on the surface of the core-shell are induced in the PL mechanism of CDs. In this purpose, the modification of CDs is used to have a control on the fluorescence emission and properties. Two aspects of functional modification have been studied including covalent and non-covalent modification[37,38].

CDs covalent modification can be related to the control of size, shape and physical properties. Involving the reaction of functional groups on CDs surface, this approach is implemented by the control of chemistry reactions. The principle of this method is to introduce or modify functional groups to increase the electron cloud density which leads to changes in the fluorescence spectrum of CDs.

One of the main reactions used for this concerns amide coupling reactions, usually called "N-doping". Nitrogen composed groups are known for their intrinsic fluorescence properties[37]. Their coupling with carboxyl groups of CDs enhances the PL emission of CDs. For example, imidazole is a common compound used in various research project that include CDs[39–41]. However, this compound has been revealed as toxic in different oxidation processes[42,43].

Related to this project, the final application aimed for is agricultural, an important feature related is the non-toxicity of the used reactants. To enhance the fluorescence of the CDs, caffeine molecules will be used.

Commonly known as caffeine, 1,3,7-trimethylxanthine is a natural compound found in coffee beans, cacao beans, or tea leaves. Recently, techniques for caffeine sensing have been developed using different fluorescence chemical detectors [44,45]. The chemical structure of caffeine (Figure. 8) shows two aromatic rings with nitrogen bonds, these structural features are the ones that allow caffeine to absorb UV light [46]. Above all, caffeine was chosen for this optimization process as it is a biobased abundant, and non-toxic additive.
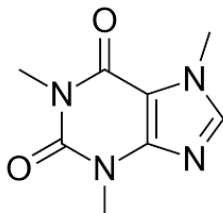

Figure 8. Chemical structure of caffeine

Non-covalent techniques of functionalization mostly refer to the electrostatic and pi-conjugated interactions that occurs between CDs and molecules. Reactions can take place via copolymerization or complexation for example. The final purpose is the same as for covalent modifications, the functionalization of the core-shell surface of CDs in adequation with the desired properties and applications.

1.4. Use of CNDs on plants

In recent years, significant improvements have been made in nanotechnology research for the agricultural field[47–49]. Particularly in enhancing the efficiency of the photosynthesis process, which is a basic requirement for all plant life. Some studies on plants using CDs proved their efficiency and positive effects. Different improvements were observed, such as improved nitrogen fixation, photosynthesis, nutrition assimilation, and enhanced plant growth[50] (Figure 9).
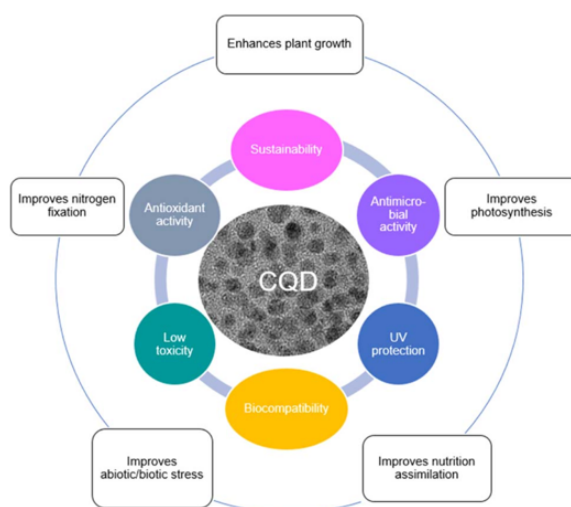

Figure 9. Properties of CQD and their effects on plants[50]

The principal reaction occurring during this process relies on the absorption of carbon dioxide by the leaves of the plants and of water by the roots, resulting in the production of oxygen and carbohydrates. Increased efficiency in this process allows plants to absorb more nutrients, resulting in more nutritious fruits and vegetables in agriculture. Besides, chlorophyll is a light-absorbing pigment present in the majority of plants that, during photosynthesis, absorbs energy from blue and red wavelengths and releases green light waves. It's for this purpose that CNDs are interesting by increasing the range of sunlight absorbance of the plants, but also by an emitting range that corresponds to chlorophyll's absorbance range [51,52]. Figure 10. presents the UV-Visible spectra of chlorophyll overlapped with the emission spectra of some SiNPs functionalized with amine groups.
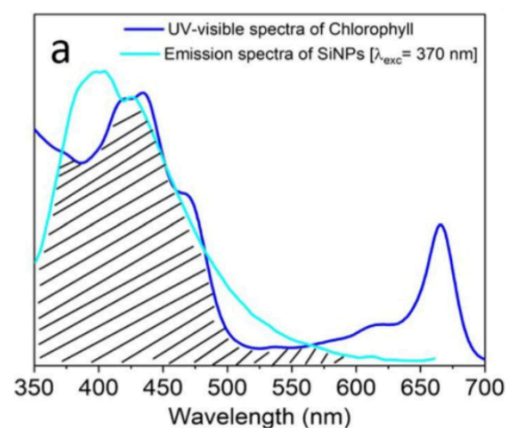

Figure 10. Spectral overlap between emission spectra of silica nanoparticles (SiNPs) with UV-Visible absorption spectrum of chlorophyll[52]

The emission spectra of the nanoparticles corresponds to the absorption range of the chlorophyll. In the case of an application of this NPs as a nano fertilizer on plants, this behavior would lead to a better absorption of the nutriments by the plants and other advantages (Figure 9).

Another aspect studied with the use of CNDs on plants is the photoprotection mechanism. Even if photosynthesis is presented as an essential process for the well-being of plants, the excess of light can have negative consequences. The main consequence is photo-oxidative damage, which leads to a decrease in photosynthesis efficiency. In fact, when a plant is exposed to an excess of light an oxidative reaction occurs on the chlorophyll, preventing the pigment from its ability to photosynthesize. In this sense, some research including the testing of CDs as nano fertilizers, proved the capacity of this nano compounds to photo protect[53,54]. Having a larger range of UV absorption than chlorophyll, the CNDs will absorb UV rays and prevent an excessing UV exposure to the treated plants. In addition, the chlorophyll pigment being protected from photo damage by the CNDs, the photosynthesis will be more efficient.

2. Aim and objectives

This work fit in with the current need of sustainable food production to assess current consequences of climate change. The main goal of this project was the development of circular carbon dots for agricultural applications. For this, versatile CNDs systems were synthesized with targeted features. This project is focused on two main aspects : enhanced photosynthesis and insect-repellency behavior.

The synthesis pathway for CNDs starts from waste biomass. The method was focused on being accessible and affordable, while reducing the use of harsh chemical compounds. With the aim of agricultural applications and once the synthesis method was determined (Figure 11.A), two steps of optimizations are presented in this work. First, the optimization of fluorescence by N-doping the CNDs with caffeine molecules (Figure 11.B). Then, a method to introduce essential oils compounds into the CNDs formulation has been developed (Figure 11.C). A combination of this two synthesis steps was then realized to obtain versatile formulations with both characteristics.

The synthesized systems were then characterized with various techniques. Photoluminescence properties were studied by fluorescence and UV-Visible spectroscopy. Composition and surface functional groups were determined by elemental analysis, FTIR and X-ray photoelectron spectroscopy. Then, a morphological approach was obtained by TEM technique. Finally, the obtained formulations were tested on insects (aphids) by the Material Science Department of the INSA of Lyon (France).
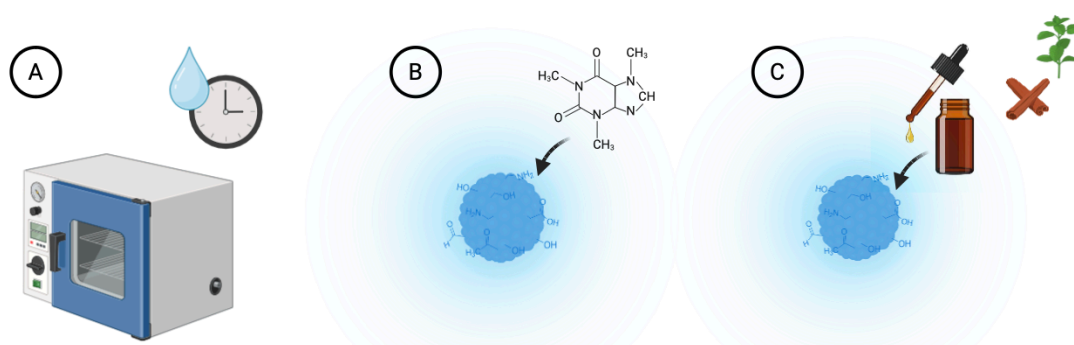

Figure 11. Schematic representation of the optimization steps followed during the project

3. Experimental part

3.1. Materials

Orange peels sourced from local shops in Donostia (Spain), were initially prepared by cutting them into pieces, washing them with distilled water, and subsequently drying for 48 hours in an oven at 60°C. The resulting dried biomass was triturated to obtain a powder. Caffeine (98% purity) was purchased from Acros Organics. Organic essential oils were provided by S.Livi and P. Da Silva (University of Lyon, France).

3.2. Preliminary tests : optimization of curing process

The optimal conditions for carbonization were determined through a series of experiments involving variations in humidity, and carbonization time. Different methods can be employed to synthesize carbon dots from biomass, one of the easiest is thermal decomposition, which consists of carbonizing the biomass at high temperature for a certain period of time. The objective of this preliminary tests was to know the effect of carbonization duration and humidity on the photoluminescence properties.

Each experiment utilized 2 g of orange peel dry powder in a glass vial, with half of the samples containing 0.6 g of water (constituting 30 % of the total mass). Carbonization was conducted at 180 °C for durations of 2, 4, and 6 hours using an oven (J.P. Selecta, Spain). A total of 6 samples was prepared (Table 1).

Table 1. Conditions of carbonization for the different test samples

Sample name	Humidity	Carbonization conditions
A_2	Dry	
B_2	30 %	2 h at 180 °C
A_4	Dry	
B_4	30 %	4 h at 180 °C
A_6	Dry	
B_6	30 %	6 h at 180 °C

The resulting carbonized biomass was dispersed in distilled water at a ratio of 100 mL per 1 g of initial biomass, followed by ultrasound treatment in three cycles of 30 minutes each, at room temperature. Subsequently, the solutions were filtrated using cotton to remove large biomass particles remaining from carbonization. Followed by a dialysis process in dialysis

tubes with a membrane of 7 kDa for 48 hours. This step of the synthesis was employed to remove particles that are smaller than the carbon dots, but the results were not as promising as expected. Another method of purification will be used in the following steps. Obtained solutions were characterized by UV-Visible spectroscopy.

3.3. N-doping with caffeine

To study the fluorescence properties of the caffeine molecule, dilutions between 1.0 and 5.0 mg/mL were prepared by dissolving pure caffeine (98 % purity) in distilled water.

For combined CNDs with caffeine, 4 systems were prepared. For each sample, 5g of dry biomass powder were added to a glass vial along with respectively 2, 5, and 10 % (wt% compared to initial biomass) of caffeine powder and 1.5 g of distilled water (30% wt.). Also, a control sample with no caffeine was prepared with the same method (Table 2).

Table 2. Sample names for N-doped optimized CNDs

Sample name	CDs	N-CDs 2%	N-CDs 5%	N-CDs 10%
Caffeine content	/	2 % wt	5 % wt	10 % wt

Carbonization was carried out in an oven at 180 °C for 6 h. Then, the carbonized biomass was dispersed in distilled water, with a ratio of 100 mL of water per gram of starting biomass. After being sonicated for 3 cycles of 30 min at room temperature, the solutions were filtered on cotton and then on a 0.45 µm nylon membrane filter. Finally, 40 mL of each solution were lyophilized for 72 h, to obtain a nanoparticle powder.

For further characterization techniques, CNDs solutions in water with different known concentrations were prepared.

3.4. Addition of essential oils

In this third part of the synthesis, the objective was to combine the previously synthetized CNDs with different essential oil (EO), to achieve an insect-repellency behavior.

Essential oils are commonly known for their medicinal properties, along as antifungal, antioxidant, antiviral and insect-repellent behaviors. Research has been made to test these

compounds as bio-repellents with low doses [55]. The previous work carried out by V.Lacotte et al. was based on the insect repellency efficiency of forty essential oils. According to their results, four of the most efficient essential oils (basil, peppermint, chinese cinnamon, greenmint) were used in this study by combination with CNDs.

The repellency properties of essential oils come from highly volatile compounds (VOCs), which are constituents of low molecular weight. The essential oils major components are displayed in Appendix 1.

Each test was done by introducing 5 g of dry biomass powder into a glass vial with 1.5 g of distilled water. The carbonization process was achieved at 180 °C for 6 h, as previously. Then, a defined amount of essential oils was added to the carbonized biomass powder. The amount of essential oil added was defined compared to the mass of biomass obtained after carbonization (1 and 2 % wt). A total of 8 systems with essential oils were prepared (Table 3).

Table 3. Sample names for insect repellent synthesized CDs, with % of EO in index

Peppermint (PP)	Basil (BA)	Greenmint (GM)	Cinnamon (CI)
$PP_{1\%}$, $PP_{2\%}$	$BA_{1\%}$, $BA_{2\%}$	$GM_{1\%}$, $GM_{2\%}$	$CI_{1\%}$, $CI_{2\%}$

The obtained mixtures of carbonized powder and oils were put in an oven at 70 °C for 2 h. The process was then the same as previously, dispersion with 100mL of distilled water per gram of starting biomass, sonification for 1.5 h at room temperature, filtration on cotton and then on a 0,45 µm nylon membrane filter , and lyophilization for 72 h.

Finally, aqueous solutions with known concentrations were prepared for further characterization purposes.

3.5. Additives-integrated systems

To combine both optimizations, synthesis methods used in parts 3.3 and 3.4 have also been combined.

A total of 8 systems were prepared (Table 4), with 5 % of caffeine for all samples, and the same amounts of EOs as previously (1 and 2 wt %), for the four different essential oils.

Table 4. Sample names for combined optimizations synthesized CDs, with 5% of caffeine and the % of EO in index

Peppermint (PP)	Basil (BA)
N-CDs$_{5\%}$ + PP$_{1\%}$, N-CDs$_{5\%}$ + PP$_{2\%}$	N-CDs$_{5\%}$ + BA$_{1\%}$, N-CDs$_{5\%}$ + BA$_{2\%}$
Greenmint (GM)	Cinnamon (CI)
N-CDs$_{5\%}$ + GM$_{1\%}$, N-CDs$_{5\%}$ + GM$_{2\%}$	N-CDs$_{5\%}$ + CI$_{1\%}$, N-CDs$_{5\%}$ + CI$_{2\%}$

As previously, 5 g of biomass along with 5 wt% of caffeine powder were placed in a vial and carbonized in an oven for 6 h at 180 °C. The obtained carbonized biomass was mixed with the essential oils and put in an oven at 70 °C for 2 h. The resulting mix was dispersed in distilled water and sonicated for 1.5 h at room temperature. Filtration on cotton and on a 0.45 µm nylon membrane was then carried out. The filtrated CNDs solutions were lyophilized for 72 h.

3.6.   Characterization techniques

Ultraviolet-visible spectroscopy (UV-Visible) is an analytical technique used to obtain information about the wavelength of UV and visible light, absorbed by the sample. The wavelength will depend on the composition of the sample. Absorption spectra were carried out on a T92+ UV-Visible Spectrophotometer (PG INSTRUMENTS) with quartz cuvette cells. Solution concentrations were adapted to the equipment calibration. Concentrations between 0,01 and 0,05 mg/mL were used for caffeine solutions. Solutions at 0,01 mg/mL in water were used for the nanoparticle solutions.

Fluorescence spectroscopy analyzes the fluorescence of a sample. Usually, an ultraviolet light is used to excite the electrons of the molecules, causing them to emit light. A Cary Eclipse Fluorescence Spectrophotometer (Agilent Technologies) was used to obtain the emission spectra, also with quartz cuvette cells. Concentrations between 0,01 and 0,05 mg/mL were used for caffeine solutions. Solutions at 0,01 mg/mL in water were used for the nanoparticle solutions.

Elemental Analysis data was provided by a Perkin Elmer Analyst 100 Atomic Absorption Spectrophotometer (Leioa, Bizkaia). The analysis of the composition based on atoms C,H and N was carried out.

Fourier-Transform Infrared Technique (FTIR) is a common analytical technique used to identify the functional groups of a compound. The resulting spectra is based on the characteristic vibration attributed to different types of bonds, under infrared irradiation. The analysis was performed on a Nicolet iS20 FTIR spectrometer, by ATR (Attenuated Total Reflection) method from 4000 to 400 nm^{-1}, with 32 scans and a resolution of 2 cm^{-1}.

X-ray photoelectron spectroscopy (XPS) is a quantitative spectroscopic technique based on surface sensitivity. Photoelectric effects are measured to identify the elements present, by applying an X-ray beam onto the sample. XPS measurements were performed on a Versaprobe III Physical Electronics (ULVAC) system with monochromatic Al Кα radiation source (1486.7 eV) (Leioa, Bizkaia). An initial analysis was carried out to determine the elements present (wide scan: step energy 0.2 eV, pass energy 224 eV) and detailed analyzes were carried out on the detected elements (detail scan: step energy 0.05 eV, pass energy 27 eV, time per step 20 ms) with an electron exit angle of 45º. The spectrometer was previously calibrated with Ag (Ag 3d5/2, 368.26 eV). The spectra were fitted using the CasaXPS 2.3.26 software, which models the contributions after a background subtraction (Shirley).

Thermogravimetric analysis (TGA) is a technique employed to determine the thermal degradation of a material, by measuring the weight loss of the sample with respect to the increasing temperature. The data was collected on a TA Instruments TGA Q500. This thermogravimetric analysis was performed in two main cycles, at first from 25°C to 800°C under nitrogen flow, and then a flow of compressed air was applied at the end of the cycle.

Transmission Electron Microscopy (TEM) is a morphological analysis that uses an electron beam to produce high resolution images of the analyzed sample on the nanoscale. The analysis was carried out on a JEOL JEM 1400 Plus microscope (Leioa, Bizkaia) with a transmission of 120kV. For this analysis the samples were solutions at 2 mg/mL of CNDs in water deposited on a subtract and left to dry.

3.7.   Application : insect-repellency tests

A series of in vitro dual-choice experiments were performed to evaluate the repellent activity of the formulations given in Table 3 and 4 against the pea aphid A. pisum. The protocol used was based on the method developed by Lacotte et al[55] with minor changes.

Bioassays were carried out in air-tight T-shaped glass tubes (shaft: 3.5 cm; head: 10 cm; diameter: 0.9 cm; volume: 7.95 cm^3) (Figure 12) in climate-controlled chambers at 20 $\pm$ 2 °C with 65 % $\pm$ 5 % RH and in the dark to avoid any possible light-related behavioral bias. Tube heads were closed on both sides by caps with an opening in the center, covered with a 40 µl pouch of liquid artificial diet sealed between two layers of Parafilm®. Artificial diets were coupled to a strip of filter paper (30 mm x 5 mm, 6.4 mg/cm^2) treated either with 10 µl of formulation for the treatment side or with the same volume of water for the control side (Figure 12).

Paper strips were impregnated 15 minutes before the start of the experiment and dried by evaporation. For formulations containing 1 % and 2 % v/v EO (i.e. 0.10 or 0.20 µl of EO at 0.94 mg/µl average density),the dose of EO applied according to the weight concentration of the paper strip was 0.98 and 1.95 % w/w, respectively, also corresponding to 0.067 or 0.13 µl/cm^2 of filter paper and 0.013 or 0.025 µl/cm^3 in the tube.
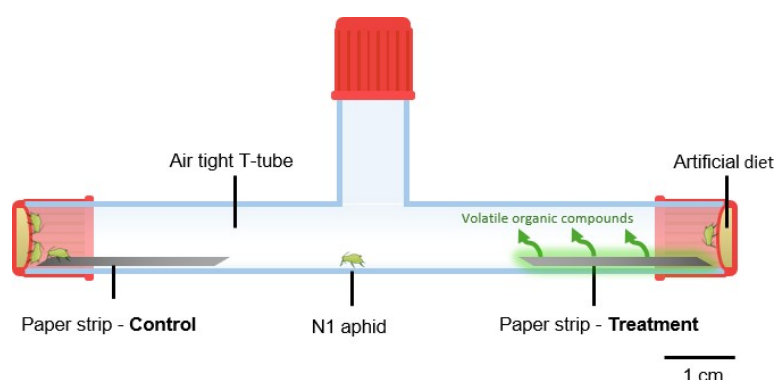

Figure 12. In vitro dual-choice T-tube for aphid repellency bioassay

Tests were initiated every day at 2 p.m. by introducing five first-instar A. pisum nymphs (N1) in the center of the tubes through the shaft. Aphids were allowed to choose a direction based on olfaction, pass beyond the paper strip (with or without physical

contact), and settle on the artificial diet. N1 aphids were preferred due to their ability to feed on an artificial diet, which allowed these tests to be performed under in vitro conditions without plant interaction.

The 'Ap3' artificial diet used in this study was specifically developed for rearing A. pisum. Twenty-four hours later, the number of aphids on each side of the tube was monitored, along with a thorough evaluation of the insects' condition. Measures were considered valid for healthy aphids settled on or located within 1 cm of the artificial diet.

All 18 formulations were tested simultaneously in five replicates. Four series of tests were performed on different dates. Therefore, for every formulation, 20 replicas and 100 aphids were tested. An equal number of blank control (water-treated filter papers on both sides of the tubes) tests were performed to validate the experimental procedure (no directional bias).

4. Results and discussion

The synthesis methodology employed was developed according to the equipment and time available for the project. Additionally, the objective of the synthesis part was to obtain a simple and reproducible method, without using harsh chemicals or organic solvents. Two ways of optimizations were also developed. The global synthesis scheme is presented in Figure 13.
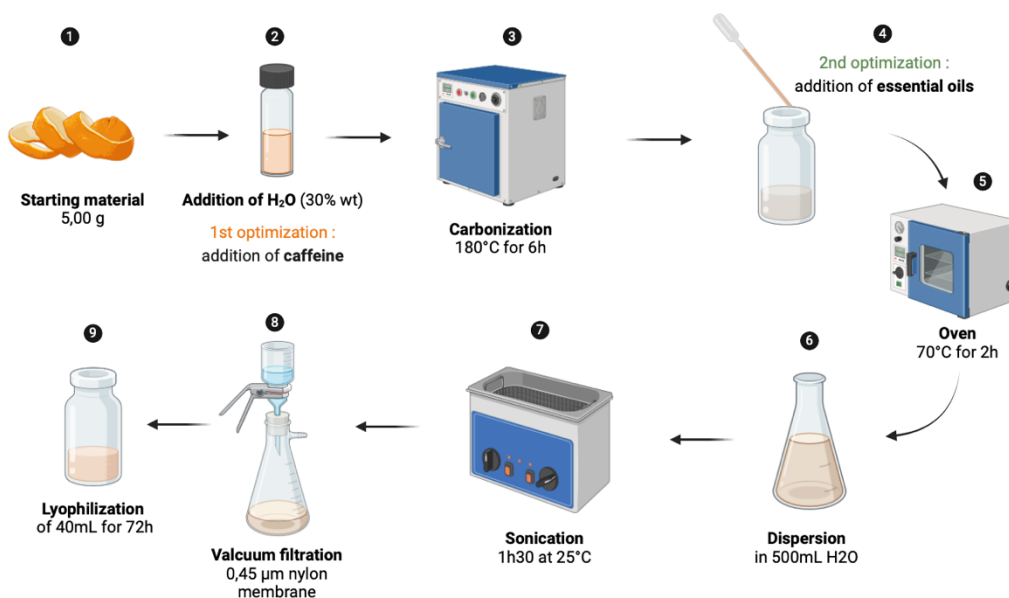

Figure 13. General synthesis pathway

To summarize, in the preliminary tests, 6 samples (A_2, A_4, A_6, B_2, B_4 and B_6) were synthesized and have been characterized only by UV-Visible spectroscopy.

In the N-doping step, 3 samples with different contents of caffeine were prepared (N-CDs 2, 5 and 10 %), in addition to a control sample without caffeine (CDs).

Four essential oils (basil, cinnamon, greenmint and peppermint) were tested at 1 and 2 % of content, resulting in 8 systems (BA 1,2 %, CI 1,2 %, GM 1,2 % and PP 1,2 %).

Finally, for the combined systems, 8 systems were prepared, all with 5% of caffeine and 1 or 2 % of the four essential oils (N-CDs 5 % + BA 1,2 %, N-CDs 5 % + CI 1,2%, N-CDs 5 % + GM 1,2 % and N-CDs 5 % + PP 1,2 %).

However, for purposes of time, the characterization techniques were carried out only for the 2 % essential oils systems. The 1 % systems were used for the insect repellency tests.

The morphological techniques were carried out for the final combined systems at 2 % of essential oils.

4.1.   Optimization of curing process

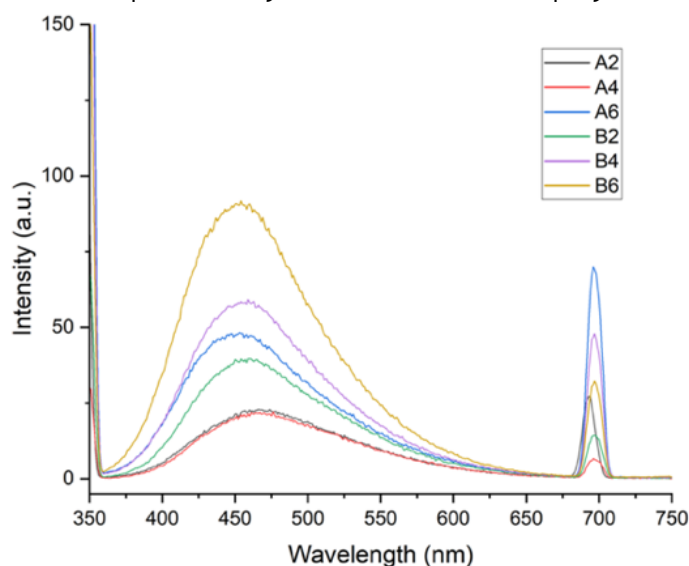UV emission spectra for the preliminary test solutions are displayed in Figure 14.

Figure 14. Emission spectra with an excitation wavelength of 350 nm of A2, A4 and A6 samples without humidity and with carbonization times of 2, 4 and 6 h, respectively, as well as B2, B4 and B6 samples with 30 % of humidity and carbonization times of 2,4 and 6 h, respectively

From this preliminary tests, the objective was to study the effect of humidity and curing carbonization time on the emission intensity of the CDs. It can be seen that a broad peak of emission appears between 400 and 575 nm, with a maximum around 460 nm, another peak of emission is noticeable at 690 nm. The intensity of the peak at 460 nm is the highest for the sample B6, with a carbonization time of 6h and a humidity of 30 % wt. In general, it can be seen that the presence of water and the increasing time of carbonization favorize the intensity of emission. Different hypothesis for this behavior can be exposed. The presence of humidity can promote hydrothermal reactions, to facilitate the breaking down of the precursors molecules, resulting in an enhance process of carbonization. Also, the possibility of the water to act as capping agent, preventing the CNDs to growth excessively, leads to a better size distribution[56].

In Figure 15, the dispersion of CNDs obtained all present blue fluorescence with different brightness. As deduced from the UV-Visible analysis, the sample B6 has the optimized conditions of preparation. This conditions of 6 h at 180 °C with 30% of humidity were the ones used for the next synthesis steps.
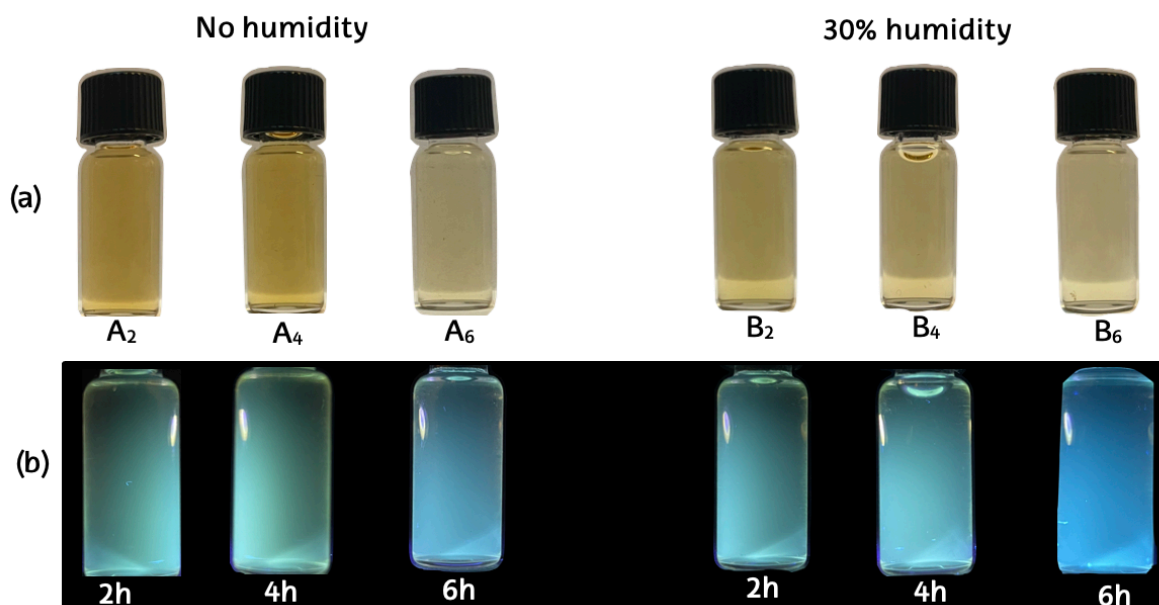
Figure 15. Preliminary CDs solutions at 1 mg/mL, (a) under sunlight and (b) under UV light (365 nm), with the conditions of carbonization used, all at 180 °C

4.2.   N-doping with caffeine

4.2.1.   Photoluminescence characterization

UV spectra of absorption and emission for the range of caffeine solutions prepared is presented in Figure 16 (a) and (b), respectively.
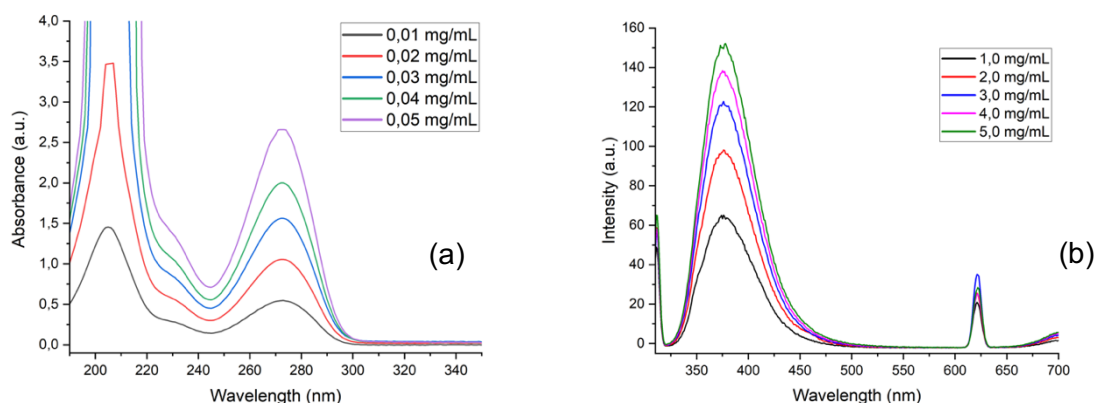

Figure 16. (a) Absorbance spectra of caffeine dilutions between 0,01 and 0,05 mg/mL, (b) Emission spectra of caffeine solutions between 1,0 and 5,0 mg/mL with an excitation wavelength of 310 nm

Two absorption peaks are observed at 205 nm and 275 nm. Emission broad peak appears from 350 to 450 nm and a slight peak at 645 nm. An increase in intensity is observed

with the increasing concentration of the caffeine solutions. For this purpose, caffeine was used to optimize the CDs fluorescence.

In the same way as previously, the absorption and emission spectra of the N-CDs systems are displayed in Figure 17.
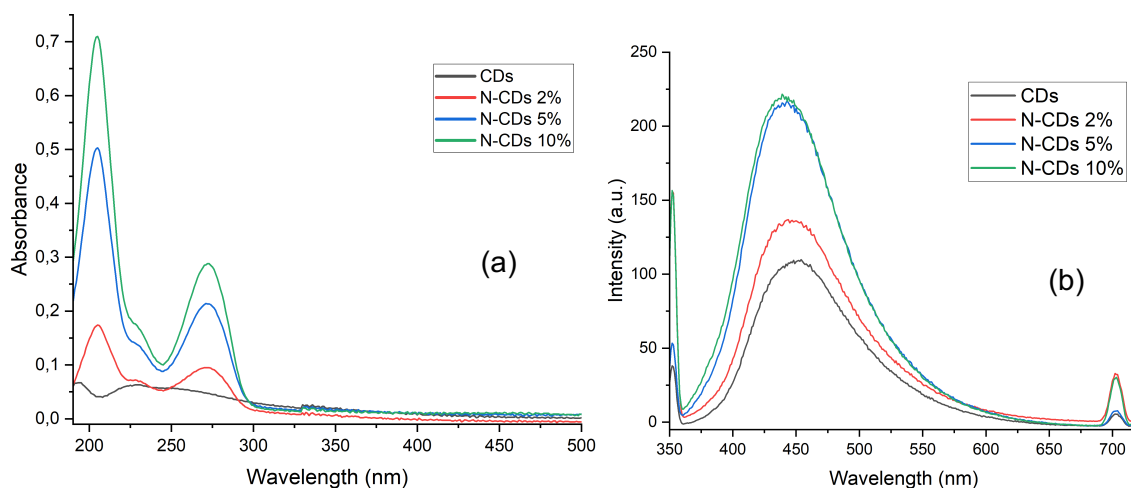
Figure 17. (a) Absorbance spectra of N-CDs solutions at 0,01 mg/mL, (b) Emission spectra of N-CDs solutions at 1,0 mg/mL with an excitation wavelength of 350 nm

Absorption spectra show two peaks for the N-CDs 2,5,10 % around 210 and 275 nm, similar to the ones of the caffeine solutions presented above. For the CDs sample a slight absorption range is noticed between 210 and 300 nm, quite less intense than the optimized fluorescence samples. For the N-CDs 2,5 and 10 %, two bands of absorption are observed at 210 and 275 nm, corresponding to transition of C=C (π-π^*) and C=O (n-π^*) bonds, respectively[57].

Emission spectra present two peaks as well, for all 4 samples, a broad peak between 400 and 575 nm and a smaller one at 700 nm. The emission intensity is noticed to increase with the increasing caffeine content in the CNDs samples. This behavior can also be observed visually in Figure 18, with a brighter blue from left to right. As the emission intensity is similar for N-CDs 5 and 10 %, for the combined systems an amount of 5 % of caffeine will be used and kept constant. Solutions of CNDs N-doped with caffeine are displayed in Figure 18.
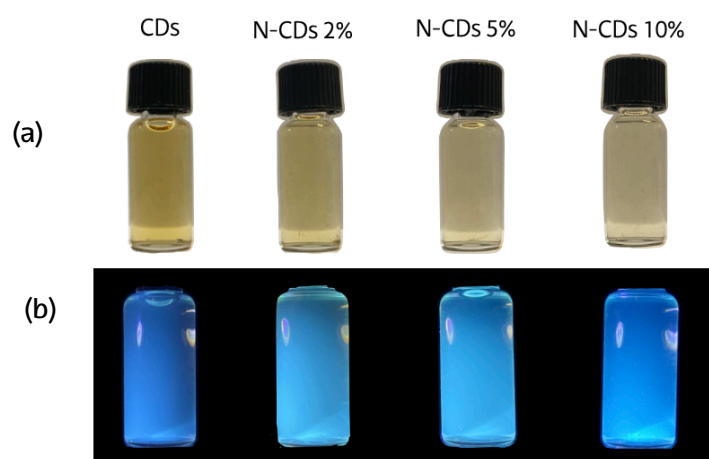
Figure 18. Solutions of N-doped CDNs, (a) under sunlight and (b) under UV light (365 nm)

4.2.2. Composition and functional groups

The structure and composition of the starting biomass, CDs and N-CDs 5 % were determined by elemental analysis, FTIR spectroscopy and X-ray photoelectron spectroscopy.

Elemental analysis results are displayed in Figure 19. The objective of this analysis was to have a quantitative idea of the biomass and CNDs composition.
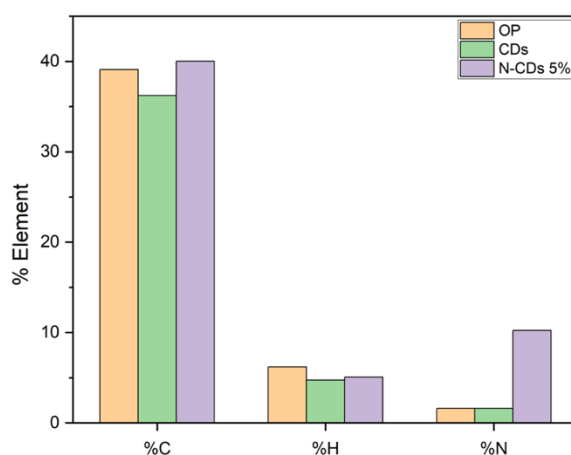

Figure 19. Percentages of C, H, N for OP, CDs and N-CDs 5 % samples, determined by elemental analysis.

The analysis confirms the presence of carbon as main element with approximately 40 % in biomass and CNDs samples. The hydrogen content is slightly lower for the CNDs compared to the biomass sample. Then, for the biomass and CDs samples, the N content was too low to be properly detected and quantified (<1.6 %). However, for the N-doped sample, the content of N reaches 10 %, proving the good integration of the N based functional groups of

the caffeine molecules. A more precise quantitative analysis is displayed by the XPS results below.

FTIR spectra of the studied samples are displayed in Figure 20. Some common absorptions peaks appear in all spectra, around 3280 cm^{-1} that can be attributed to OH bonding, and peaks at 2864 and 2970 cm^{-1} can be related to C-H bonding stretching vibrations. The absorption peaks present at 1350 cm^{-1} reveals the presence of C-O bonds. Narrow peaks between 1643 and 1733 cm^{-1}, present in all three spectra can be attributed to aliphatic C=O bending.
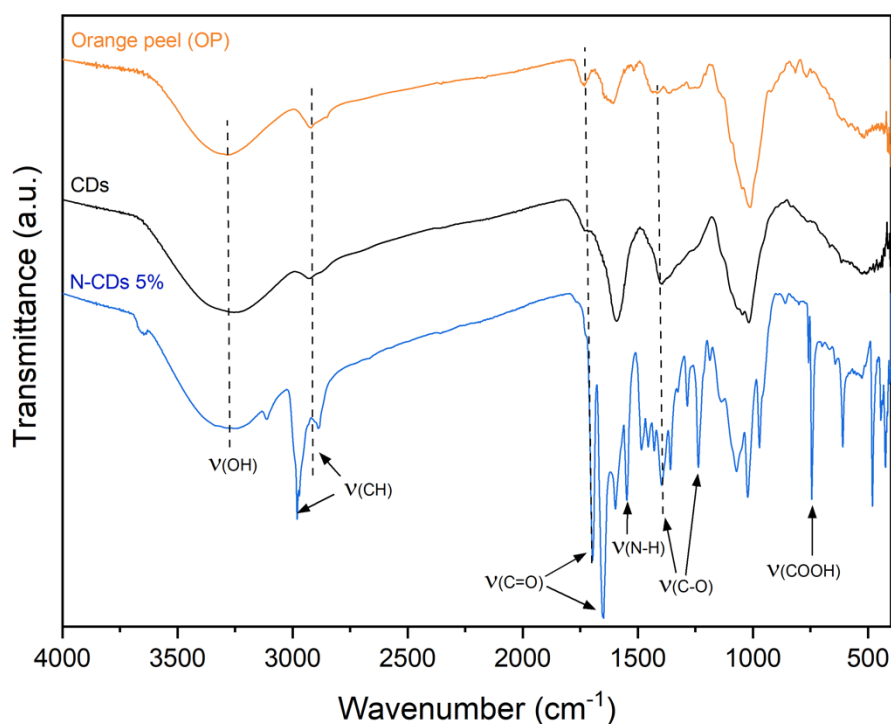
Figure 20. FTIR spectra of OP (orange peels), CDs and N-CDs 5 %

Additionally, for the N-doped sample, the broad peak around 3280 cm^{-1} can also be attributed to N-H bonding. The broad peak observed around 3280 cm^{-1} is more intense for the N-CDs 5 % samples that contains caffeine. This sample also presents amide functional groups with N-H stretching, C=O stretching, NH bending and C-O stretching bonds (3280, 1692, 1540 and 1235 cm^{-1} respectively). Moreover, secondary amides are indicated by the C-N stretching at 1270 cm-1, along with the peaks of NH bending (1540 cm^{-1}) and C=O stretching (1648 cm^{-1}). Finally, the intense narrow peak at 740 cm^{-1} can be attributed to carboxylic acid groups.

In brief, FTIR revealed the presence of different oxygenated functional groups such as hydroxyl, carbonyl and carboxyl for the three samples. The N-doped sample present additional N-based functional groups, due to the modification with the caffeine compound.

XPS analysis was conducted to confirm the FTIR and elemental analysis results. From the table results of XPS (Table 5), the main elements present are C and O. For the N-CDs 5 % sample, the presence of N was also detected, for the OP and CDs sample the amount of N presented is an approximation, due the proximity with the background.

The presence of other compounds in limited amounts can also be appreciated such as К, Cl and Si for the CDs sample. The N-doped sample also presents some К content.

Table 5. Percentages of C, N and O elements with corresponding functional groups for OP, CDs and N-CDs 5 % samples, determined by XPS measurements

Entry	OP	CDs	N-CDs 5%
% C	**75.6**	**60.5**	**60.0**
C–C/C–H	40.42	24.23	17.59
C–O/C–N	23.39	25.19	27.76
C=O	8.67	9.15	10.84
O–C=O/N–C=O	3.15	1.88	3.81
% N	**1.3***	**1.3***	**3.4**
NH$_2$	0.99*	1.3*	/
C–N–C	/	/	3.4
N–C$_3$	0.34*	/	/
% O	**22.4**	**30.7**	**33.3**
C=O	1.43	5.73	7.36
C–OH	18.72	22.05	22.09
O=C–O	2.28	2.9	3.83
%К	/	3.4	2.5
%Cl	/	1.0*	/
%Si	/	2.6*	/

* Approximated values due to the proximity with background noise

The OP sample presents 75 % of carbon content, which confirms the choice of this biomass waste as precursor for the synthesis of carbon dots. Samples CDs and N-CDs 5 % are composed of approximatively 60 % of carbon and 30 % of oxygen.

To determine the surface functional groups of the samples, the deconvoluted spectra of C1s, O1s and N1s are presented in Figure 21.
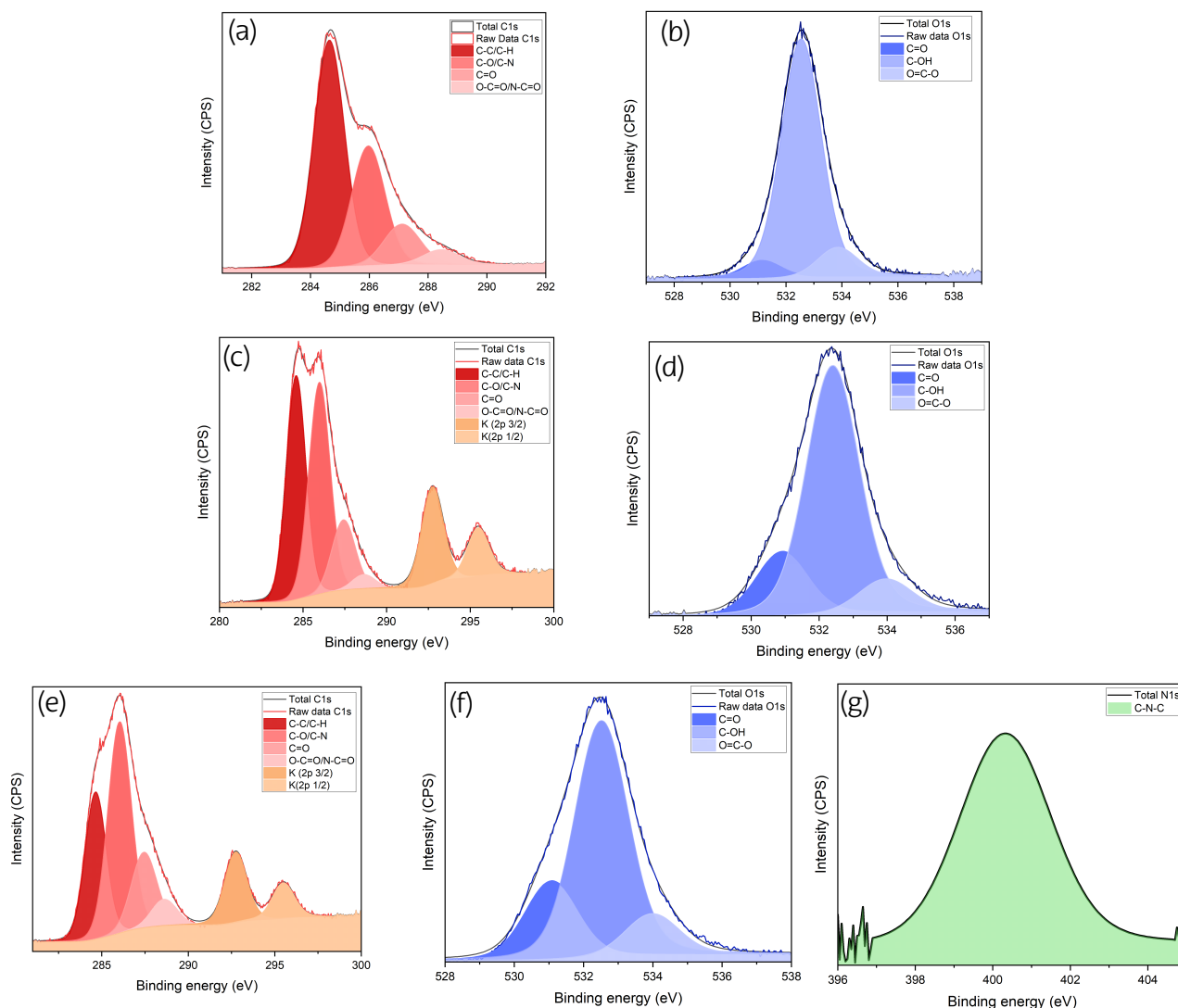

Figure 21. Deconvoluted C1s and O1s spectra for (a,b) OP sample, (c,d) CDs sample, (e,f) for N-CDs 5 % with also N1s deconvoluted (e) for N-CDs 5 % sample

The deconvolutes curves of C1s corresponds to C-C /C-H at 284.6 eV, C-O/C-N at 286.0 eV, C=O at 287.1 eV and O-C=O/N-C=O at 288.5 eV. For the CDs and N-CDs 5 % samples, the results also show the presence of К, at 292.7 and 295.5 eV.

Bonds resulting from the O1s deconvoluted spectra are attributed to C=O, C-OH and O=C-O, at 531.0, 532.4 and 539.9 eV, respectively.

From the N1s deconvoluted spectra of the N-CDs 5 % sample, the binding energy at 400.3 eV indicates the presence of C-N-C bonds. XPS results corroborates the functional groups determined by FTIR analysis.

Thermogravimetric analysis was carried out to study the behavior of the CNDs with temperature. From XPS analysis, results show that CNDs are mostly composed of carbon (60 %) and oxygen (30 %) and small amounts of minerals (К, Si). The TGA resulting curves are displayed in Figure 22.
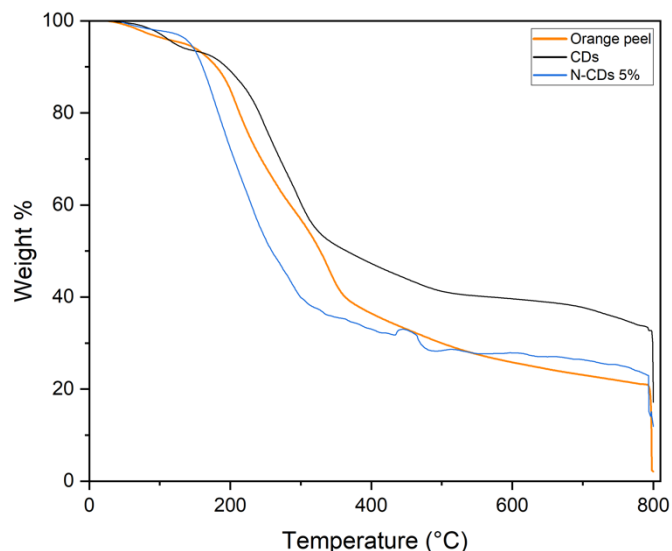

Figure 22. TGA curves for OP, CDs and N-CDs 5 %

From the thermal decomposition process achieved, a water loss can be observed up to 200 °C for all samples. The event occurring between 200 and 300 °C can be mainly attributed to the loss of CO_2 and could also be due to the depolymerization and decarbonylation of products containing hydroxyl, carbonyl and carbon bonds.

The residue mass percentage at 800 °C was also measured resulting in 1.53, 11.73 and 8.88 %, for OP, CDs and N-CDs 5 % samples, respectively. For the biomass sample (OP), the residue is very low, certainly corresponding to few minerals that XPS analysis could not detect. For the CNDs samples, the residue measured may correspond to the carbon particle, as well as an inorganic part composed of minerals from the biomass.

4.3.   Essential oils systems

4.3.1.   *Photoluminescence characterization*

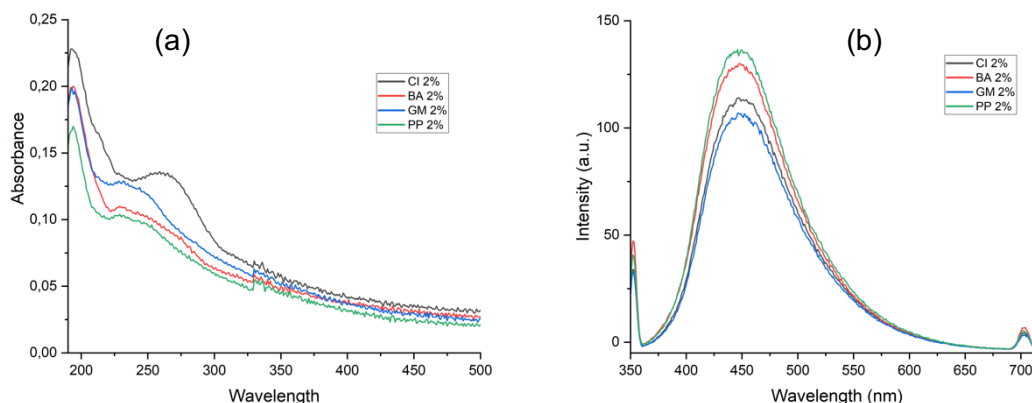UV-visible spectroscopy results for the essential oil optimized samples are presented in Figure 23.

Figure 23. (a) Absorbance spectra of EO optimized CDs solutions at 0,01 mg/mL, (b) Emission spectra of EO optimized CDs at 1,0 mg/mL with an excitation wavelength of 350 nm

In Figure 23 (a), two absorptions bands appear at 195 and 265 nm, the intensity of the peaks observed is lower than for the caffeine optimized samples in Figure 17. Also, in (b) the emission peaks observed are in the same range as previously, between 400 and 575 nm, with a maximum intensity of emission at 455 nm. It can also be noticed that the relative emission intensity is higher for these samples containing essential oils (same solution concentration), comparing to the CDs sample (Figure 17), meaning that the addition of essential oils slightly accentuated the PL properties of the CNDs systems. The sample with the highest emission intensity appears to be the peppermint essential oil CNDs even if no visible trend appears between the absorption and emission results. Solutions obatined are presented in Figure 24.
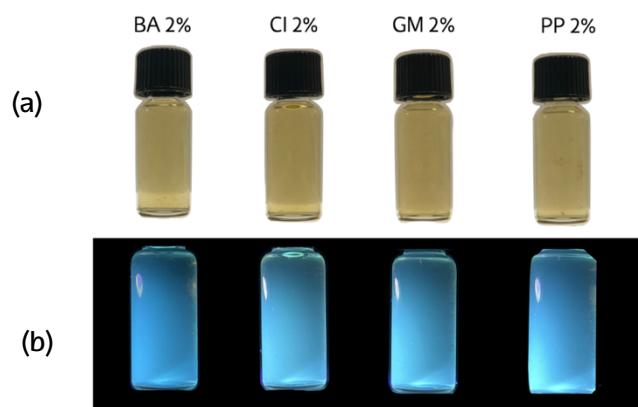

Figure 24. Solution of CNDs samples with 2 % of essential oil at 1 mg/mL, (a) under sunlight and (b) under UV light (365nm)

4.3.2. Composition and functional groups

As well as for the previous samples, FTIR, XPS and elemental analysis techniques were carried out to study the composition of the CNDs with essential oils.

Displayed in Appendix 1, the main components of the four essential oils tested (basil, cinnamon, greenmint and peppermint) present terpenoid structures, which can be presented as carbon cycles with or without double bonds, with oxygenated groups.

Different composition analysis techniques are displayed (elemental analysis, FTIR and XPS) to study the integration of the essential oils' functional groups into the CNDs.

Elemental analysis results are presented in Figure 25. The composition of the four systems is quite similar, even if the synthesis employed different essential oils. Carbon content is comprised between 34 and 39 %. As expected, the amount of nitrogen wasn't properly detected by the analysis as it is very low ($< 1.6\%$). These samples does not contain caffeine or any other compound that could include nitrogen functional groups.
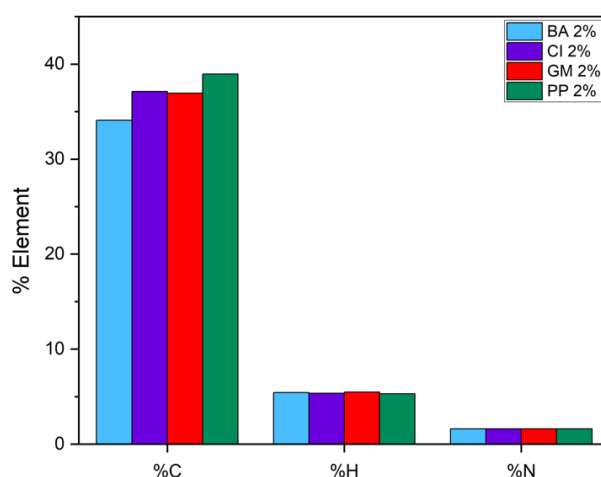

Figure 25. Percentages of C, H, N for essential oil systems, determined by elemental analysis

The FTIR results for BA 2 %, CI 2 %, GM 2 % and PP 2 % samples are displayed in Figure 26. The four spectra present similar absorptions bands. However, slight differences in the intensity of absorption can be observed. As in the previous FTIR spectra of CNDs, the two peaks at 2981 and 2885 cm^{-1} indicate the CH stretching band, a much less intense broad band at 3308 cm^{-1} is attributed to hydroxyl functional groups. A particular band appears at 3662 cm^{-1} which could be attributed to some inorganic minerals (Si, K, P) present in the CNDs systems, this assumption will be confirmed by XPS analysis.
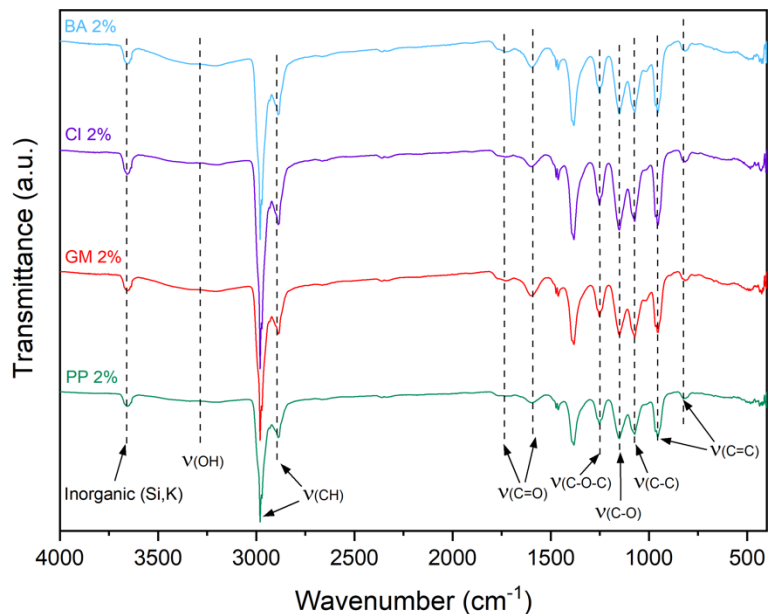
Figure 26. FTIR spectra of essential oil systems

Additionally, typical groups present in the essential oil components can be observed as carbonyl (1602 and 1752 cm^{-1}), symmetric and asymmetric CH_2 and CH_3 signals (1383 and 1464 cm^{-1}), acetate asymmetric stretching (1252 cm^{-1}), C-O and C-C bonds (1148 and 1071 cm^{-1}, respectively, and C=C bonds (952 and 813 cm^{-1}).

The FTIR analysis revealed the expected composition proposing similitudes with the CDs sample analysis (Figure 20), and also by presenting some of the main functional groups that compose the VOCs of the essential oils (Appendix 1).

To confirm the surface functional groups present, XPS analysis was conducted, to corroborate FTIR conclusions. Results of XPS analysis are detailed in Table 6. The composition of the four samples is very similar, with a carbon content between 58 and 68 %, oxygen content between 25 and 29 %. Very low N content is reported as it is an approximation due to the binding energy which is close to the background noise.

Different minerals contents are presented such as K, Si, Na, S and P, this correlates with the FTIR absorption band observed around 3660 cm^{-1} in Figure 26.

Table 6. Percentages of C, N and O elements with corresponding functional groups for essential oil systems, determined by XPS measurements

Entry	BA 2%	CI 2%	GM 2%	PP 2%
%C	58.3	68.0	64.5	66.5
C–C/C–H	37.9	38.73	30.52	43.54
C–O/C–N	15.86	21.95	23.72	16.85
C=O	3.43	5.01	7.39	4.48
O–C=O/N–C=O	1.13	2.29	2.87	1.66
%N	0.9*	1.6*	1.1*	1.2*
NH$_2$	0.9*	1.33*	1.1*	1.2*
N–C$_3$	/	0.29*	/	/
%O	29.4	26.3	29.7	25.5
C=O	11.15	2.81	3.85	9.67
C–OH	18.21	23.52	23.7	15.84
O=C–O	/	/	2.1	/
%К	4.5	1.1	1.5	2.5
%Si	3.8	2.7	3.0	1.6
%Na	0.6*	/	/	0.3*
%S	1.9	/	0.3*	0.7*
%P	0.5*	/	/	0.6*

* Approximated values due to the proximity with background noise

The binding energies for the different functional groups are the same as the ones described in part 4.3.2, and the deconvoluted curves are displayed in Figure 27. Even if the four essential oils have different volatile organic compounds, the functional groups are similar. Carbonyl and hydroxyl functional groups present the higher amounts within all.

In the C1s deconvoluted curves presented, the binding energies correspond to hydrogen, carbonyl and acetate bonds. On the C1s deconvoluted curves, the presence of hydroxyl and carbonyl groups is confirmed. Also, a difference in intensity of the binding energies can be observed. For the CNDs with greenmint essential oil (GM 2 %), the area corresponding to the binding energy of the C–O and C–N is more intense corresponding to 23.72 %, therefore the PP 2 % sample presents only 16.85 %.

Also, from the O1s deconvoluted curves, the presence of carbonyl and hydroxyl groups is confirmed.

By comparison with the FTIR results above, XPS analysis corroborates the surface functional groups present in the essential oils CNDs systems.
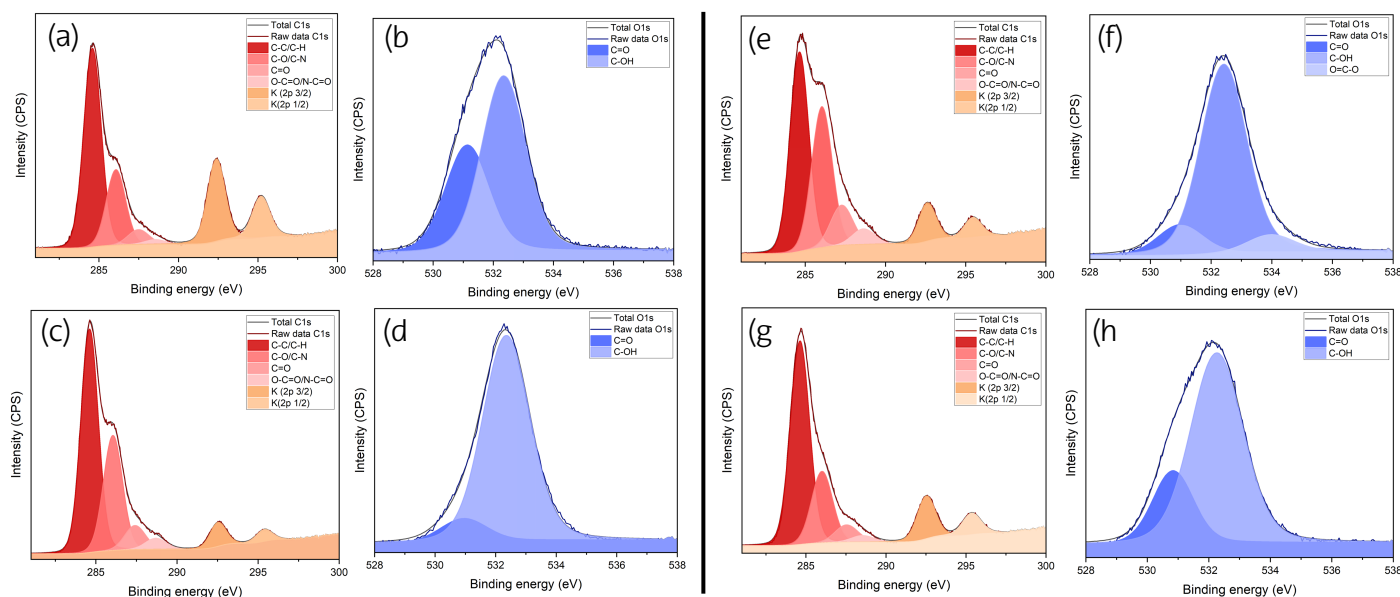
Figure 27. Deconvoluted C1s and O1s spectra for (a,b) BA 2 %, (c,d), CI 2 %, (e,f) GM 2 % and (g,h) PP 2 %

Thermogravimetric analysis results exposing the weight % loss as a function of temperature are displayed in Figure 28. In the same way as previously, a water loss is observed until 200 °C and then with a higher slope, the CO_2 loss. The various CNDs with essential oils samples present very similar curves, however a difference is noticeable with the thermal decomposition of the biomass. The biomass weight loss is similar until 350 °C, and becomes more important until 800 °C.
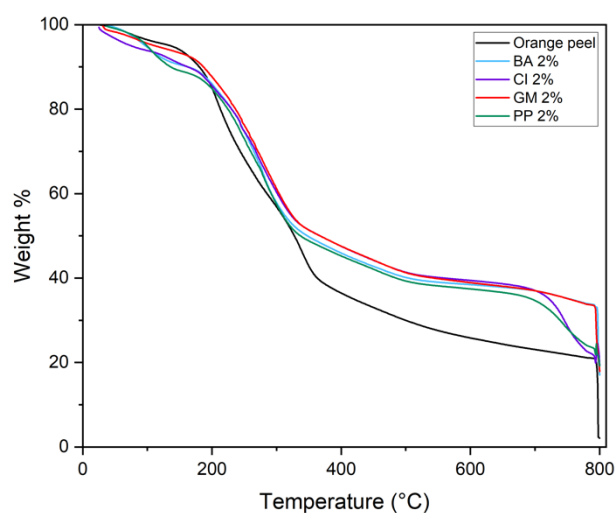
Figure 28. TGA curves for CDs systems for essential oils systems

The final residue measured is of 11.38, 9.80, 9.15 and 8.79 %, for BA 2 %, CI 2 %, GM 2 % and PP 2 % samples, respectively. As for the biomass and CDs systems, this residue can

hypothetically be attributed to the minerals present and confirmed by FTIR and XPS analysis, but also to the carbon core shell part of the CNDs.

The different composition analysis carried out confirm the integration of the essential oil principal groups into the CNDs, an important behavior for the insect-repellency test carried out.

4.4.   Additives-integrated systems

4.4.1.   Photoluminescence properties

Figure 29. displays the optical UV-visible results for the combined optimizations systems. The systems all contain 5 % of caffeine and 2 % of essential oil.
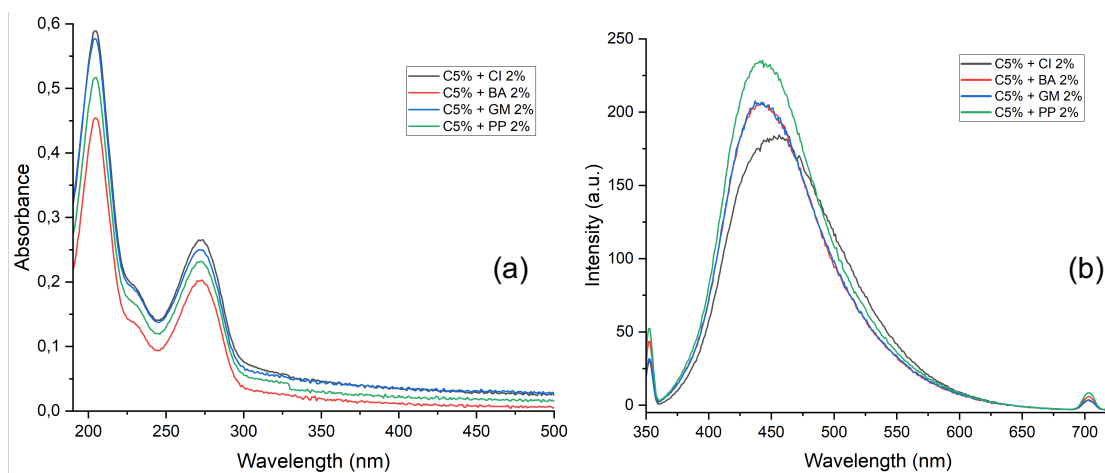
Figure 29. (a) Absorbance spectra of combined systems samples at 0,01 mg/mL, (b) Emission spectra of combined systems at 1,0 mg/mL with an excitation wavelength of 350 nm

Absorption bands are shifted to longest wavelengths compared to the essential oil CNDs, with two peaks at 210 and 275 nm. This bands are the same as the one for the caffeine optimized samples. Emission band appears between 400 and 575 nm, with N-CDs 5 % + PP 2 % sample as the most intense one, coinciding with previous results.

Again, no correlation can be made between the absorption trend and the emission one. However, the relative intensity of the emission bands is higher than the one of the essential oils systems displayed in Figure 23.

The objective of this combined systems was to combine the useful aspects of both fluorescence optimization with caffeine, and the functional groups of essential oils. This behavior will be confirmed with the composition analysis below.

Obtained solutions are displayed in Figure 30. A bright blue fluorescence can be observed in all the samples.
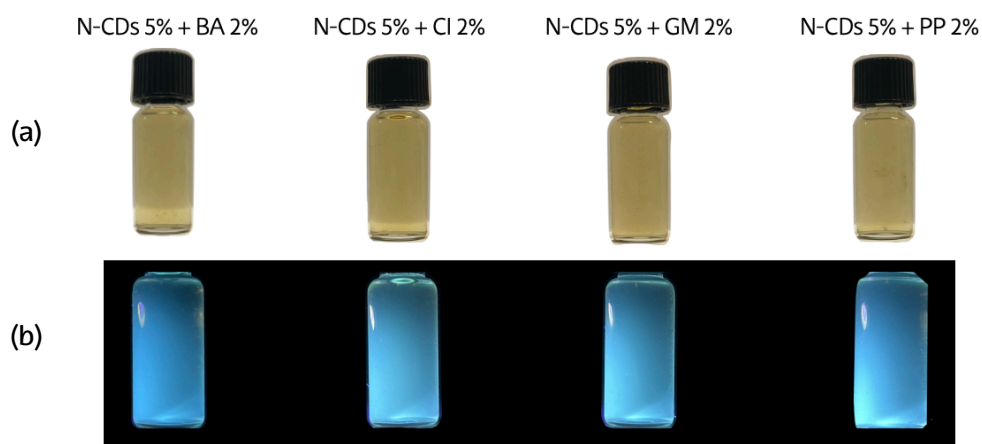

Figure 30. Solution of CNDs combined systems samples with 5% of caffeine and 2% of essential oil at 1 mg/mL, (a) under sunlight and (b) under UV light (365nm)

4.4.2. Composition and functional groups

Combined systems composition was analyzed by elemental analysis, FTIR and XPS analysis.

Elemental analysis results are presented in Figure 31. As in previous results, the main element detected is carbon with a slightly higher content than in essential oils systems (Figure 25), reaching more than 40 %. The modification with caffeine is confirmed with the detection of N in all samples, approximately 10 % in content.
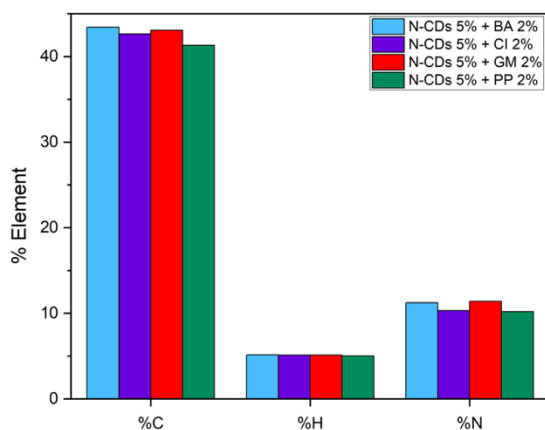

Figure 31. Percentages of C, H, N for combined systems samples, determined by elemental analysis

These combined systems present, as for the essential oils systems, present very similar FTIR spectra (Figure 32). The intensity of the absorption bands are also very similar. As for the other FTIR spectra displayed, the absorption band at 3327 cm^{-1} is attributed to the OH stretching, the bands at 2944 and 2879 cm^{-1} corresponds to CH stretching. Carbonyl groups are assumed by the absorption peaks at 1649 and 1697 cm^{-1}. From the N-doping modification process with caffeine, the presence of NH bending at 1548 cm^{-1} and C-N bonds at 1453 cm^{-1} is assumed. Aromatic rings are indicated by the combination of absorption peaks at 1600, 1491 and 1432 cm^{-1}. C-O stretching group and acetate are attributed with bands at 1353 and 1243 cm^{-1}, respectively. Finally, the absorption band at 746 cm-1 can be attributed to carboxylic acid functional group.
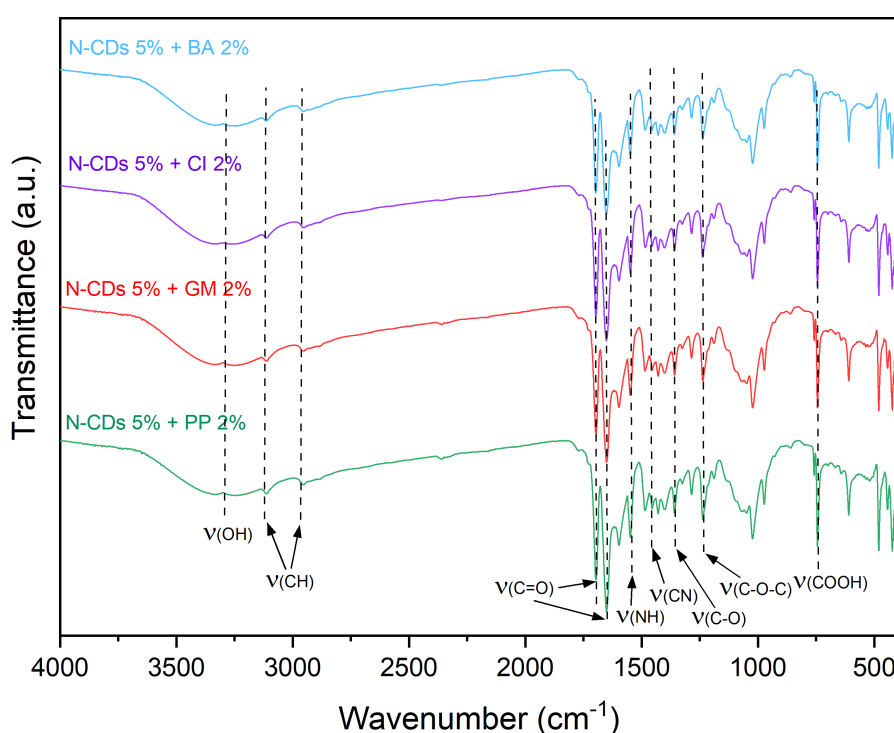

Figure 32. FTIR spectra of combined systems samples

XPS detailed results for combined systems are displayed in Table 3, along with the C1s, O1s and N1s deconvoluted spectra in Figure 33. For these samples, the main elements present in the samples are C (~65 %), O (~30 %) and the presence of N is confirmed more than 3 % in each sample. Composition and functional groups percentages are consistent between samples.

For these combined systems, the results do not show the presence of various minerals as previously, only an approximated small amount of S was detected in N-CDs 5 % + BA 2 % and N-CDS 5 % + CI 2 % samples.

Table 7. Percentages of C, N and O elements with corresponding functional groups for combined systems samples, determined by XPS measurements

Entry	N-CDs 5 % + BA 2 %	N-CDs 5 % + CI 2 %	N-CDs 5 % + GM 2 %	N-CDs 5 % + PP 2 %
% C	65.2	63.8	64.0	66.0
C-C/C-H	25.08	23.2	22.2	25.51
C-O/C-N	26.56	26.37	28.44	27.07
C=O	9.32	9.71	9.19	9.63
O-C=O/N-C=O	4.19	4.54	4.21	3.82
% N	3.5	3.2	3.4	3.5
% O	29.6	30.6	31.4	28.7
C=O	6.3	6.58	5.7	6.23
C-OH	19.56	20.5	21.95	17.95
O=C-O	3.69	3.54	3.7	4.55
%К	1.5	1.9	1.3	1.6
%S	0.3*	0.3*	/	/

* Approximated values due to the proximity with background noise

The main bonds resulting from this XPS analysis are C-C/C-H, C-O/C-N and C-OH, confirming the FTIR spectra results. Other common bonds from essential oil VOCs, like C=O and O-C=O can be appreciated from the O1s deconvoluted spectra. The binding energies measured are the same as in part 4.3.2.

The N-doping modification is confirmed with the presence of C-N-C bonds at 400.2 eV in all the combined systems samples. From the O1s deconvoluted samples, the presence of C=O, C-OH and C=O-C is admitted. It can be noticed here that the intensities are very similar between the samples.
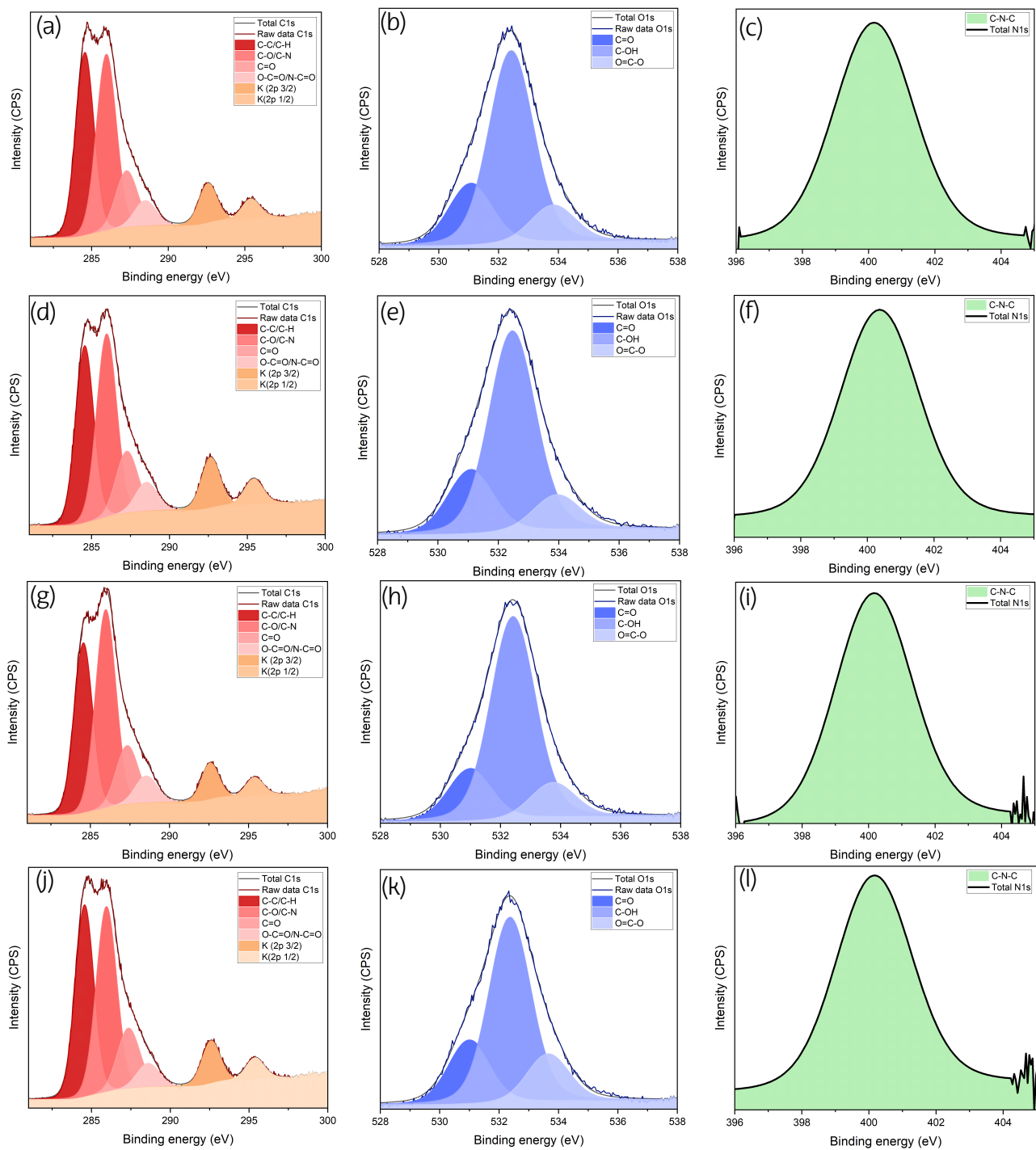
Figure 33. Deconvoluted C1s, O1s and N1s spectra for (a,b,c) N-CDs + BA 2 %, (d,e,f) N-CDs + Cl 2 %, (g,h,i) N-CDs + GM 2 % and (j,k,l) N-CDs + PP 2 %, respectively

TGA results for the combined systems are displayed in Figure 34. The behavior of the weight % with temperature is similar to the one observed for the N-doped samples and essential oils CNDs. The water loss occurs until 200 °C, followed by a higher decrease in weight due to the loss of CO_2. The curves of the combined systems follow the same pattern. However, compared to the biomass, the weight loss is more consequent for the combined systems between 150 and 500 °C.
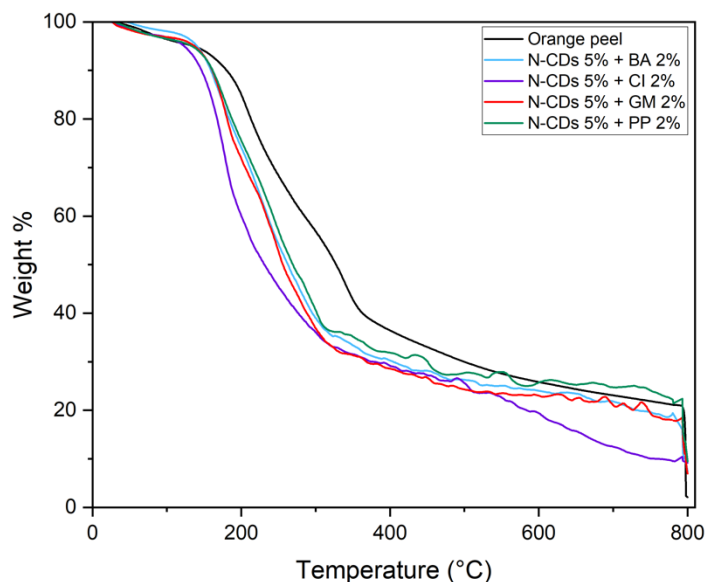
Figure 34. TGA curves of combined systems samples and biomass

The measured residues at 800 °C corresponds to 5.5, 7.3, 6.3 and 7.7 % wt for N-CDs + BA 2 %, N-CDs + CI 2 %, N-CDs + GM 2 % and N-CDs + PP 2 %, respectively. As discussed in part 3.4.2, this residue corresponds to the carbon particles, and also to the few minerals detected. As the amount of minerals detected by XPS analysis is lower for these combined systems than for the essential oils one, the residue values are somehow lower.

The composition analysis of the combined systems showed the charcateristics of both modification processes. The addition of caffeine is well noticed with the high emission fluorescence and the appearance of N functional groups. Additionally, the essential oils VOCs present a good integration as the main functional groups are present on the CNDs surface.

4.4.3. Morphological analysis

Transmission electron microscopy (TEM) was employed to study the morphological features of the carbon dots. Figure 35 displays the obtained images as well as a size distribution resulting.
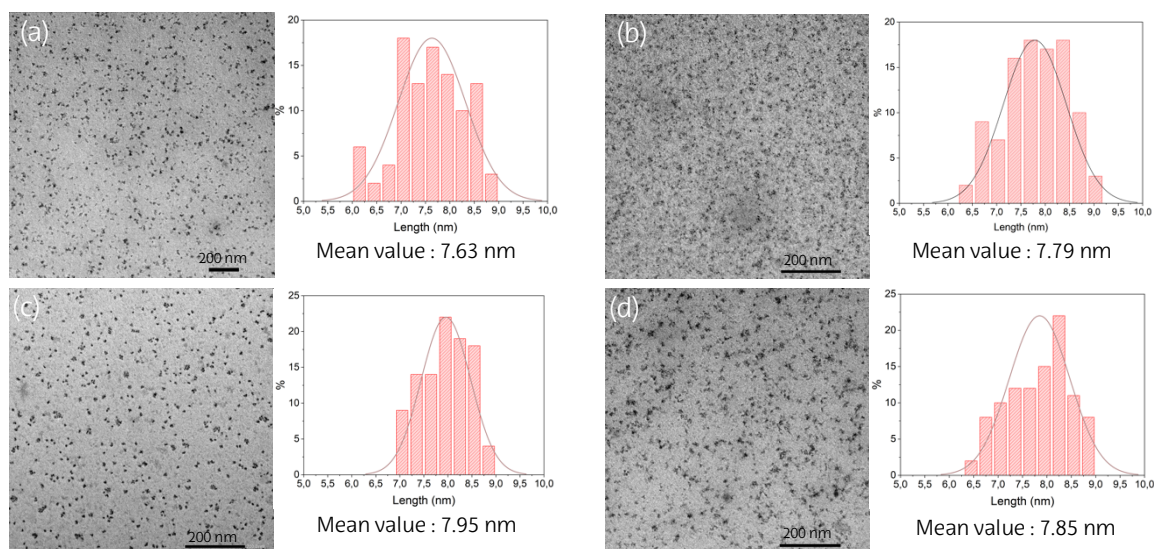

Figure 35. (a), (b),(c),(d) TEM images obtained, along with size distribution corresponding for N-CDs 5% + BA 2%, N-CDs 5% + CI 2%, N-CDs 5% + GM 2% and N-CDs 5% + PP 2% samples, respectively

The dots can be well observed in the resulting images, with some small aggregations appearing. The average size goes between 7.6 and 7.9 nm, with distribution sizes going from 6.1 to 8.9 nm. The CNDs display a near-spherical morphology. The distribution is more or less uniform. The size distribution is narrow, going from 6.0 nm for the smaller CNDs to 9.0 nm for the larger ones. This morphological analysis confirms the formation of CNDs.

4.5. Insect-repellency tests

It is important to highlight that this insect-repellency study is based on a statistical analysis which is detailed in Appendix 2. The results of the in vitro dual choice experiment are shown in Figure 36.
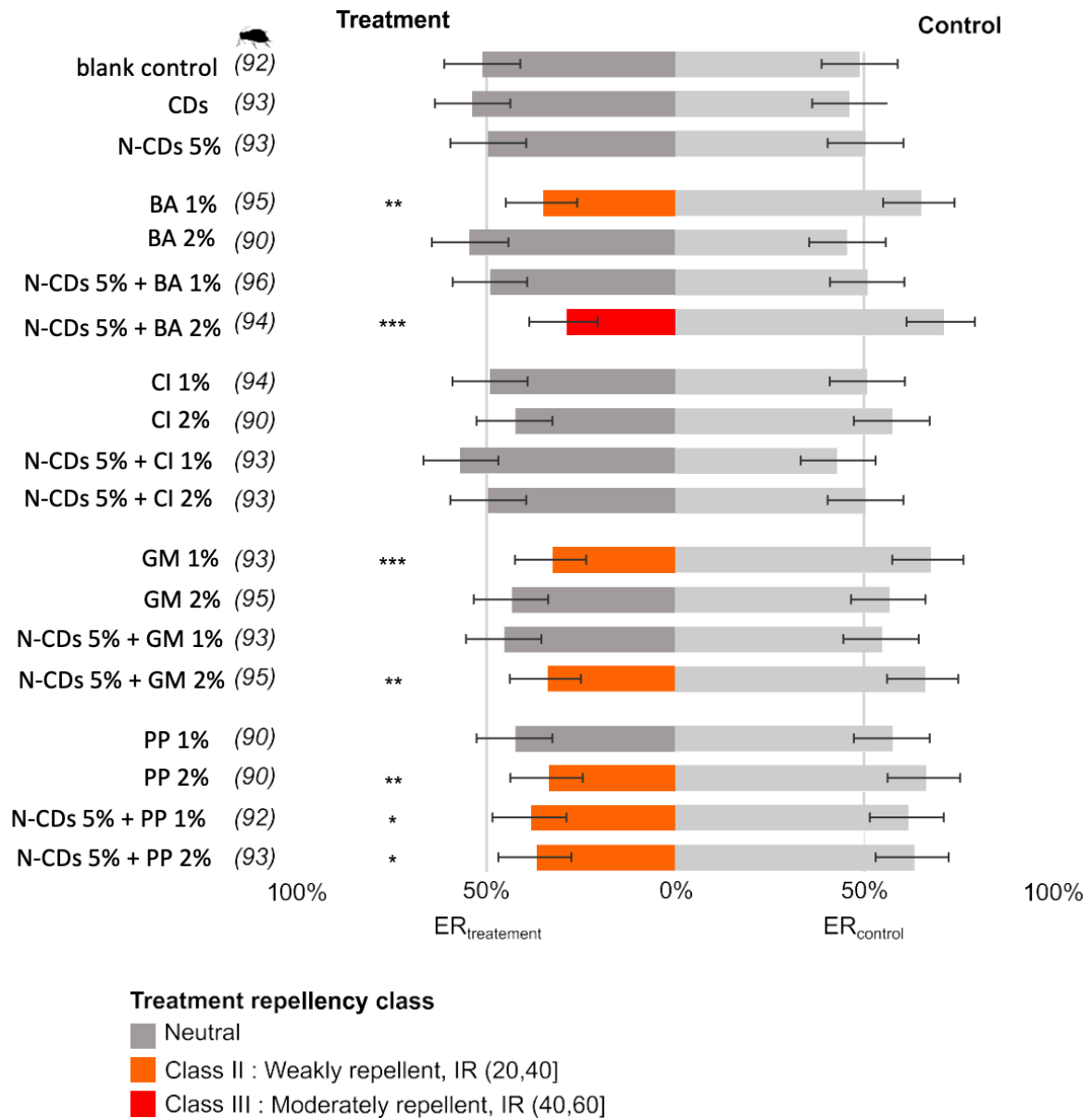

Figure 36. Results of the insect repellency tests illustrated by the insects' average establishment rate between artificial diet and control or treatment side. Total number of valid measures obtained per treatment is indicated within brackets

Control tests using water as treatment (blank control) were carried out to validate the test procedure. The results showed nostatistically significant deviation in *A. pisum*

behavior compared with equal distribution and random choice where ERcontrol = ERtreatment = 0.5) (P › 0.05) and, thus, no directional bias within the experimental setup.

Tests using CD nanoparticles alone (CDs) and CD nanoparticles added with 5 % wt caffeine (N-CDs 5 %) were carried out to assess the aphids' response to CDs and caffeine, respectively. Similarly to the blank control, the results of these tests showed no significant difference in aphid preference between the two directions (P › 0.05), indicating that the base components of the formulations, CDs or N-CDs 5%, have no impact on the insect's behavior.

EO-based formulations showed either statistically significant repellency (P ‹ 0.05) or no impact on aphid behavior (P › 0.05), with no specific pattern regarding the EO tested (basil, cinnamon, green mint or peppermint) and its concentration (1 or 2 % wt) or the addition of caffeine (no caffeine or 5 % wt). To investigate these effects, the choice of aphids was then analyzed using a generalized linear model (GLM) with EO, EO concentration and caffeine concentration set as explanatory variables (fixed effects). However, results showed a complex, significant tripartite interaction between these three factors ($\chi^2(3) = 13.4$, P ‹ 0.001), which has not been investigated further.

Six formulations containing basil, green mint and peppermint were classified as 'weakly repellent' according to their repellency index (RI%): N-CDs 5% + PP 1% (23.9), N-CDs 5% + PP 2% (26.9), BA 1% (30.5), N-CDs 5% + GM 2% (32.6), PP 2% (33.3), GM 1% (35.5). One formulation was classified as 'moderately repellent': N-CDs 5% + BA 2% (42.6). The other formulations, including those based on cinnamon, were classified as "neutral", with no impact on aphid preference.

5. Conclusions

In this project, a methodology for the synthesis of CNDs from waste biomass was successfully developed. The synthesis was based on a thermal decomposition process followed by sonication, filtration and lyophilization steps.

The preliminary step implied the optimization of the carbonization process. From the UV-visible analysis carried out, the optimized conditions resulted in the highest time of carbonization and the use of water in small amounts for the carbonization step. With the aim of enhancing the photosynthesis process in plants, the first optimization step implied a modification by N-doping with caffeine was demonstrated. The addition of caffeine in the synthesis process allowed the N-CNDs to nearly double the absorption and emission fluorescence intensity. From the composition analysis, the presence of the biomass functional groups (hydroxyl, carbonyl, acetate) was reported in the CNDs samples. In addition, for the N-doped sample, the presence of amide and urethane groups confirmed the integration of the caffeine functional group on the surface of the CNDs. The second optimization step required the integration of four different essential oils in the CNDs synthesis process. This functionalization demonstrated expected results as the groups composing the VOCs of the essential oils were reported in the composition analysis. Also, it can be noticed that the absorption and emission was still remarkable for this essential oils systems. Then, the combination of these optimizations was carried out to combine the desired features. The characterization results were coherent with the previously mentioned optimizations. Resulting in an improved fluorescence and the integration of the essential oils functional groups. The morphological analysis revealed highly uniform, monodisperse CNDs, each with a spherical shape and a diameter of about 7.6 nm, highlighting the consistency of the proposed synthesis method.

Finally, the insect repellence tests carried out gave encouraging results for an innovative CNDs system. It is important to note that the amount of essential oil is very low. Some of the synthesized systems revealed a weakly or moderate repellent activity.

Further perspectives can include a continuity in the insect repellent tests with new formulations containing more essential oils in order to get an eventual correlation. These CNDs have been fully characterized, revealing exceptional properties and potential benefits for crop growth. The next phase involves field testing these carbon dots on orange crops to validate their effectiveness in enhancing plant growth and resilience, thereby completing a circular "orange-to-orange" cycle. This innovative approach not only aims to reduce agricultural waste but also promotes a sustainable, closed-loop system, paving the way for greener, more productive farming practices.

6. Conclusiones

En este proyecto se desarrolló con éxito una metodología para la síntesis de CNDs a partir de biomasa residual. La síntesis se basó en un proceso de descomposición térmica seguido de etapas de sonicación, filtración y liofilización.

El paso preliminar implicó la optimización del proceso de carbonización. A partir del análisis UV-visible realizado, las condiciones optimizadas dieron como resultado el mayor tiempo de carbonización y el uso de agua en pequeñas cantidades para el paso de carbonización. Con el objetivo de mejorar el proceso de fotosíntesis en las plantas, se demostró que el primer paso de optimización implicaba una modificación por dopaje de N con cafeína. La adición de cafeína en el proceso de síntesis permitió que los N-CNDs casi duplicaran la intensidad de absorción y emisión de fluorescencia. Del análisis de composición se desprende la presencia de los grupos funcionales de la biomasa (hidroxilo, carbonilo, acetato) en las muestras de CNDs. Además, para la muestra dopada con N, la presencia de grupos amida y uretano confirmó la integración del grupo funcional cafeína en la superficie de los CNDs. El segundo paso de optimización requirió la integración de cuatro aceites esenciales diferentes en el proceso de síntesis de los CNDs. Esta funcionalización demostró los resultados esperados, ya que los grupos que componen los COVs de los aceites esenciales fueron reportados en el análisis de composición. Además, puede observarse que la absorción y la emisión seguían siendo notables para estos sistemas de aceites esenciales. A continuación, se llevó a cabo la combinación de estas optimizaciones para aunar las características deseadas. Los resultados de la caracterización fueron coherentes con las optimizaciones mencionadas anteriormente. El resultado fue una fluorescencia mejorada y la integración de los grupos funcionales de los aceites esenciales. El análisis morfológico reveló CNDs altamente uniformes y monodispersos, cada uno con una forma esférica y un diámetro de aproximadamente 7,6 nm, destacando la coherencia del método de síntesis propuesto.

Por último, las pruebas de repelencia de insectos realizadas arrojaron resultados alentadores para un sistema innovador de CNDs. Es importante señalar que la cantidad de aceite esencial es muy baja. Algunos de los sistemas sintetizados revelaron una actividad repelente débil o moderada.

Otras perspectivas pueden incluir una continuidad en los ensayos de repelencia de insectos con nuevas formulaciones que contengan más aceites esenciales para obtener una eventual correlación. Estos CNDs han sido completamente caracterizados, revelando propiedades excepcionales y beneficios potenciales para el crecimiento de los cultivos. La siguiente fase consiste en probar sobre el terreno estos puntos de carbono en cultivos de naranjas para validar su eficacia en la mejora del crecimiento y la resistencia de las plantas,

completando así un ciclo circular "de la naranja a la naranja". Este planteamiento innovador no sólo pretende reducir los residuos agrícolas, sino también promover un sistema sostenible de circuito cerrado, allanando el camino hacia una agricultura más ecológica y productiva.
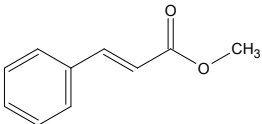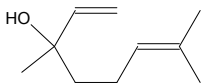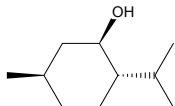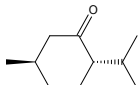
7. References
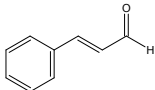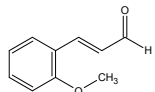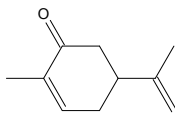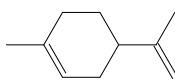
1. THE 17 GOALS | Sustainable Development. https://sdgs.un.org/goals.
2. AR6 Synthesis Report: Climate Change 2023. https://www.ipcc.ch/report/ar6/syr/.
3. CLIMATE CHANGE 2023 Synthesis Report A Report of the Intergovernmental Panel on Climate Change. doi:10.59327/IPCC/AR6-9789291691647.
4. 2023 GAP Report | Virginia Tech CALS Global. https://globalagriculturalproductivity.org/2023-gap-report/.
5. Tilman, D., Balzer, C., Hill, J. & Befort, B. L. Global food demand and the sustainable intensification of agriculture. Proc Natl Acad Sci U S A 108, 20260–20264 (2011).
6. Zhang, W. J. Integrated pest management and pesticide use. in Integrated Pest Management: Pesticide Problems, Vol.3 1–46 (Springer Netherlands, 2014). doi:10.1007/978-94-007-7796-5_1.
7. Khan, Md. A. & Ahmad, W. Synthetic Chemical Insecticides: Environmental and Agro Contaminants. in 1–22 (2019). doi:10.1007/978-3-030-23045-6_1.
8. Khan, M. A. et al. Insect pest resistance: An alternative approach for crop protection. in Crop Production and Global Environmental Issues 257–282 (Springer International Publishing, 2015). doi:10.1007/978-3-319-23162-4_11.
9. Pesticides and Soil Health. https://www.biologicaldiversity.org/campaigns/pesticides-and-soil-health/.
10. (PDF) Mechanisms and strategies for pesticide biodegradation: Opportunity for waste, soils and water cleaning. https://www.researchgate.net/publication/287245972_Mechanisms_and_strategies_for_pesticide_biodegradation_Opportunity_for_waste_soils_and_water_cleaning.
11. Thavaseelan, D. & Priyadarshana, G. Nanofertilizer use for Sustainable Agriculture. JOURNAL OF RESEARCH TECHNOLOGY AND ENGINEERING 2, (2021).
12. Bhardwaj, R. L., Parashar, A., Parewa, H. P. & Vyas, L. An Alarming Decline in the Nutritional Quality of Foods: The Biggest Challenge for Future Generations' Health. Foods 13, (2024).
13. Mayer, A. M. B., Trenchard, L. & Rayns, F. Historical changes in the mineral content of fruit and vegetables in the UK from 1940 to 2019: a concern for human nutrition and agriculture. Int J Food Sci Nutr 73, 315–326 (2022).
14. Gomollón-Bel, F. Ten Chemical Innovations That Will Change Our World: IUPAC identifies emerging technologies in Chemistry with potential to make our planet more sustainable. Chemistry International 41, 12–17 (2019).
15. Xu, X. et al. Electrophoretic analysis and purification of fluorescent single-walled carbon nanotube fragments. J Am Chem Soc 126, 12736–12737 (2004).
16. Liu, J., Li, R. & Yang, B. Carbon Dots: A New Type of Carbon-Based Nanomaterial with Wide Applications. ACS Cent Sci 6, 2179–2195 (2020).
17. Ozyurt, D., Kobaisi, M. Al, Hocking, R. K. & Fox, B. Properties, synthesis, and applications of carbon dots: A review. Carbon Trends 12, 100276 (2023).
18. Ross, S., Wu, R. S., Wei, S. C., Ross, G. M. & Chang, H. T. The analytical and biomedical applications of carbon dots and their future theranostic potential: A review. J Food Drug Anal 28, 677 (2020).
19. Ghirardello, M., Ramos-Soriano, J. & Galan, M. C. Carbon dots as an emergent class of antimicrobial agents. Nanomaterials vol. 11 Preprint at https://doi.org/10.3390/nano11081877 (2021).

20. Schweizer, T., Kubach, H. & Koch, T. Investigations to characterize the interactions of light radiation, engine operating media and fluorescence tracers for the use of qualitative light-induced fluorescence in engine systems. Automotive and Engine Technology 6, 275–287 (2021).

21. Yan, F. et al. The fluorescence mechanism of carbon dots, and methods for tuning their emission color: a review. doi:10.1007/s00604-019-3688-y.

22. Zhang, Q., Wang, R., Feng, B., Zhong, X. & Ostrikov, K. (Ken). Photoluminescence mechanism of carbon dots: triggering high-color-purity red fluorescence emission through edge amino protonation. Nature Communications 2021 12:1 12, 1–13 (2021).

23. Fernando, K. A. S. et al. Carbon quantum dots and applications in photocatalytic energy conversion. ACS Appl Mater Interfaces 7, 8363–8376 (2015).

24. Ai, L. et al. 2007523 (1 of 31) Efficient Combination of G-C 3 N 4 and CDs for Enhanced Photocatalytic Performance: A Review of Synthesis, Strategies, and Applications. (2021) doi:10.1002/smll.202007523.

25. Kong, J. et al. molecules Carbon Quantum Dots: Properties, Preparation, and Applications. (2024) doi:10.3390/molecules29092002.

26. Kurian, M. & Paul, A. Recent trends in the use of green sources for carbon dot synthesis-A short review. Carbon Trends 3, 32 (2021).

27. Mansuriya, B. D. & Altintas, Z. Carbon Dots: Classification, Properties, Synthesis, Characterization, and Applications in Health Care-An Updated Review (2018-2021). 11 (2018) doi:10.3390/nano.

28. Bourlinos, A. B. et al. Carbogenic nanoparticles Surface Functionalized Carbogenic Quantum Dots**. 4, 455–458 (2008).

29. Ge, G. et al. Carbon dots: synthesis, properties and biomedical applications. J. Mater. Chem. B 9, 6553–6575 (2021).

30. Deshmukh, M. A., Park, S. J., Hedau, B. S. & Ha, T. J. Recent progress in solar cells based on carbon nanomaterials. Solar Energy 220, 953–990 (2021).

31. Perli, G. et al. Synthesis of Carbon Nanodots from Sugarcane Syrup, and Their Incorporation into a Hydrogel-Based Composite to Fabricate Innovative Fluorescent Microstructured Polymer Optical Fibers. Gels 8, (2022).

32. Sattariazar, S., Arsalani, N. & Nejad Ebrahimi, S. Biological assessment of synthesized carbon dots from polyphenol enriched extract of pomegranate peel, incorporated with Mentha piperita essential oil. Mater Chem Phys 294, 126981 (2023).

33. Wareing, T. C., Gentile, P. & Phan, A. N. Biomass-Based Carbon Dots: Current Development and Future Perspectives. ACS Nano 15, 15471–15501 (2021).

34. Jing, H. H. et al. Green Carbon Dots: Synthesis, Characterization, Properties and Biomedical Applications. Journal of Functional Biomaterials 2023, Vol. 14, Page 27 14, 27 (2023).

35. Electrónico, C. MINISTERIO DE AGRICULTURA, PESCA Y ALIMENTACIÓN Nota de prensa.

36. Rivas, B., Torrado, A., Torre, P., Converti, A. & Domínguez, J. M. Submerged citric acid fermentation on orange peel autohydrolysate. J Agric Food Chem 56, 2380–2387 (2008).

37. Yan, F. et al. Surface modification and chemical functionalization of carbon dots: a review. doi:10.1007/s00604-018-2953-9.

38. Wang, H. et al. Surface Modification Functionalized Carbon Dots Chemistry-A European Journal. Chem. Eur. J. 2023 29, 202302383–202302384 (2023).

39. Yang, D. et al. Functionalization of citric acid-based carbon dots by imidazole toward novel green corrosion inhibitor for carbon steel. J Clean Prod 229, 180–192 (2019).

40. Ye, Y., Yang, D. & Chen, H. A green and effective corrosion inhibitor of functionalized carbon dots. J Mater Sci Technol 35, 2243–2253 (2019).

41. Wang, X. et al. Imidazole derivative-functionalized carbon dots: using as a fluorescent probe for detecting water and imaging of live cells. 44, 5547 (2015).

42. Siciliano, A. et al. Chronic toxicity of treated and untreated aqueous solutions containing imidazole-based ionic liquids and their oxydized by-products. Ecotoxicol Environ Saf 180, 466–472 (2019).

43. Evjen, S. et al. Degradative Behavior and Toxicity of Alkylated Imidazoles. (2019) doi:10.1021/acs.iecr.9b05100.

44. Xu, W. et al. Make Caffeine Visible: a Fluorescent Caffeine '"Traffic Light"' Detector. (2013) doi:10.1038/srep02255.

45. Tasić, Ž. Z., Petrović Mihajlović, M. B., Simonović, A. T., Radovanović, M. B. & Antonijević, M. M. Recent Advances in Electrochemical Sensors for Caffeine Determination. Sensors vol. 22 Preprint at https://doi.org/10.3390/s22239185 (2022).

46. Weldegebreal, B., Redi-Abshiro, M. & Chandravanshi, B. S. Development of new analytical methods for the determination of caffeine content in aqueous solution of green coffee beans. Chem Cent J 11, (2017).

47. Wang, C. et al. Nitrogen-Doped Carbon Dots Increased Light Conversion and Electron Supply to Improve the Corn Photosystem and Yield. Environ. Sci. Technol 55, 25 (2021).

48. Swift, T. A. et al. Photosynthesis and crop productivity are enhanced by glucose-functionalised carbon dots. New Phytologist 229, 783–790 (2021).

49. Guirguis, A. et al. Boosting Plant Photosynthesis with Carbon Dots: A Critical Review of Performance and Prospects. (2023) doi:10.1002/smll.202300671.

50. Abu Salha, B., Saravanan, A., Maruthapandi, M., Perelshtein, I. & Gedanken, A. Plant-Derived Nitrogen-Doped Carbon Dots as an Effective Fertilizer for Enhanced Strawberry Growth and Yield. ACS ES and T Engineering 3, 1165–1175 (2023).

51. Xu, X. et al. Improving Plant Photosynthesis through Light-Harvesting Upconversion Nanoparticles. ACS Nano 16, 18027–18037 (2022).

52. Singh, V., Mandal, T., Mishra, S. R., Singh, A. & Khare, P. Development of amine-functionalized fluorescent silica nanoparticles from coal fly ash as a sustainable source for nanofertilizer. Scientific Reports | 14, 3069 (123AD).

53. Hu, C. et al. Synthesis of modified carbon dots with performance of ultraviolet absorption used in sunscreen. Optics Express, Vol. 27, Issue 5, pp. 7629-7641 27, 7629–7641 (2019).

54. Jing, X. et al. Enhanced photosynthetic efficiency by nitrogen-doped carbon dots via plastoquinone-involved electron transfer in apple. Hortic Res 11, (2024).

55. Lacotte, V. et al. Bioactivity and chemical composition of forty plant essential oils against the pea aphid Acyrthosiphon pisum revealed peppermint oil as a promising biorepellent. Ind Crops Prod 197, (2023).

56. Czerwińska, K., Śliz, M. & Wilk, M. Hydrothermal carbonization process: Fundamentals, main parameter characteristics and possible applications including an effective method of SARS-CoV-2 mitigation in sewage sludge. A review. Renewable and Sustainable Energy Reviews 154, 111873 (2022).

57. Hjort, R. G. et al. Carbon dots using a household cleaning liquid as a dopant for iron detection in hydroponic systems †. (2023) doi:10.1039/d3ra01713c.

8. Appendix

Appendix 1. Main VOCs of the four essential oils tested

Essential oil tested	Main components	Chemical structure
Basil	Methyl chavicol 90%	
	Linalool 7.9%	
Peppermint	Menthol 43%	
	Menthone 34%	
Chinese cinnamon	Trans-cinnamaldehyde 92%	
	2-methoxy-cinnamaldehyde 5.8%	
Green mint	Carvone 81%	
	Limonene 14%	

Appendix 2. Statistical analysis for insect repellency activity tests

Insect preference was compared to an equal distribution using exact binomial tests with the null hypothesis that an aphid would choose either side of the test tubes with equal probability (0.5). The response variable is expressed as the average establishment rate of aphids on the control side of the tubes ($ER_{control}$) given by the formula (a), where i is the replicate number, N is the total number of replicates performed and Nb.control and Nb.treatment are the number of aphids established on or within 1 cm of the artificial diets on the control and treatment sides, respectively.

The analysis only included aphids that settled on either side of the test tube, meaning that $ER_{control}$ + $ER_{treatment}$ = 1, where $ER_{treatment}$ is the average establishment rate on the treatment side. Under the H_0 null hypothesis that an aphid would choose either side with an equal probability, $ER_{control}$ = $ER_{treatment}$ = 0.5. Conversely, under the H_1 alternative hypothesis that an aphid would preferentially choose one side, $ER_{control} \neq ER_{treatment} \neq 0.5$.

$$(a)\ ER_{control} = \frac{\sum_{i=1}^{N}(\text{Nb. control})}{\sum_{i=1}^{N}(\text{Nb. control} + \text{Nb. treatment})}$$

For a given treatment, when aphids preferentially chose one side, we calculated a repellency index (%) (RI), according to formula (b) (McDonald et al., 1970), that is linearly related to $ER_{control}$ as follows: RI = ($2ER_{control}$ -1)*100. Positive (>0) and negative (<0) RI values indicate repulsive and attractive effects, respectively.

$$(b)\ RI = \frac{\sum_{i=1}^{N}(\text{Nb. control}) - \sum_{i=1}^{N}(\text{Nb. treatment})}{\sum_{i=1}^{N}(\text{Nb. control} + \text{Nb. treatment})} * 100$$

The RI of treatments was grouped in relative repellency classes according to the classification presented in Table X adapted from Lacotte et al. and initially proposed by McDonald et al. (McDonald et al., 1970). When aphids showed no preference, treatments were classified as 'Neutral'.

Table X. Relative repellency classes of treatments

Hypothesis		Classes	Repellency Index (%)	Property of the treatment
H_0: $ER_{control} = ER_{treatment} = 0.5$		0	-	Neutral
H_1: $ER_{control} \neq ER_{treatment} \neq 0.5$		V	(80,100]	Very repellent
		IV	(60,80]	Repellent
		III	(40,60]	Moderately repellent
		II	(20,40]	Weakly repellent
		I	(0,20]	Very weakly repellent
		-I	[-20,0)	Very weakly attractive
		-II	[-40,-20)	Weakly attractive
		-III	[-60,-40)	Moderately attractive
		-IV	[-80,-60)	Attractive
		-V	[-100,-80)	Very attractive

Insect preference was compared to an equal distribution using an exact binomial test. Significance: $P < 0.001$: ***, $P < 0.01$: **, $P < 0.05$: *. If aphids preferentially chose one side ($P < 0.05$), the treatment was grouped into arepellency class according to its repellency index (RI (%) = [(C − T)/(C + T)] × 100 where C is thetotal number of aphids on the control side, and T is the total number of aphids on the treatment side). In the opposite case ($P > 0.05$), the treatment was classified as "neutral". Twenty groups of five first instar nymphs (<1 day old, N1) were tested per treatment (100 N1 in total).